PP2018-RA-01469 Revised

Article type: Research Article

Short title: Phosphate starvation alters root calcium signatures

Author for Contact: Julia M. Davies

Article title: Phosphate starvation alters abiotic-stress-induced cytosolic free calcium increases in roots

Authors: Elsa Matthus[1], Katie A. Wilkins[1], Stéphanie M. Swarbreck[1], Nicholas H. Doddrell[1,a], Fabrizio G. Doccula[2], Alex Costa[2,3], Julia M. Davies[1]

Affiliations:

[1] Department of Plant Sciences, University of Cambridge, Downing Street, Cambridge CB2 3EA, UK.

[2] Department of Biosciences, University of Milan, Via G. Celoria 26, 20133 Milan, Italy.

[3] Institute of Biophysics, Consiglio Nazionale delle Ricerche, Via G. Celoria 26, 20133 Milan, Italy.

One-sentence summary: Phosphate starvation, but not nitrogen starvation, changes the cytosolic free calcium signatures of *Arabidopsis thaliana* roots in response to mechanical, salt, osmotic, and oxidative stress, as well as to extracellular nucleotides.

Author contributions: E.M. and J.M.D. conceived the project. E.M., K.A.W., S.M.S., F.G.D., A.C., and J.M.D. designed the experiments. E.M., F.G.D, and N.H.D. carried out the experiments and analyzed the data. E.M. and J.M.D. wrote the article with contributions from all the authors. J.M.D. agrees to serve as the author responsible for contact and ensures communication.

Funding information: BBSRC Doctoral Training Programme (BB/J014540/1) and the Broodbank Trust. Ministero dell'Istruzione dell'Università e della Ricerca, Fondo per gli Investimenti della Ricerca di Base (FIRB) 2010 RBFR10S1LJ_001. University of Milan Transition Grant - Horizon 2020, Fondo di ricerca Linea 1A Progetto "Unimi Partenariati H2020" and Piano di Sviluppo di Ateneo 2016, 2017.

Present addresses:

[a] National Institute of Agricultural Botany East Malling Research (NIAB EMR), New Road, East Malling ME19 6BJ, UK.

Email address of Author for Contact: jmd32@cam.ac.uk

ABSTRACT

Phosphate (Pi) deficiency strongly limits plant growth, and plant roots foraging the soil for nutrients need to adapt to optimize Pi uptake. Ca^{2+} is known to signal in root development and adaptation but has to be tightly controlled as it is highly toxic to Pi metabolism. Under Pi starvation and the resulting decreased cellular Pi pool, the use of cytosolic free Ca^{2+} ($[Ca^{2+}]_{cyt}$) as a signal transducer may therefore have to be altered. Employing aequorin-expressing Arabidopsis (*Arabidopsis thaliana*), we show that Pi starvation, but not nitrogen starvation, strongly dampens the $[Ca^{2+}]_{cyt}$ increases evoked by mechanical, salt, osmotic, and oxidative stress as well as by extracellular nucleotides. The altered root $[Ca^{2+}]_{cyt}$ response to extracellular ATP manifests during seedling development under chronic Pi deprivation but can be reversed by Pi resupply. Employing ratiometric imaging, we delineate that Pi-starved roots have a normal response to extracellular ATP at the apex but show a strongly dampened $[Ca^{2+}]_{cyt}$ response in distal parts of the root tip, correlating with high reactive oxygen species (ROS) levels induced by Pi starvation. Excluding iron, as well as Pi, rescues this altered $[Ca^{2+}]_{cyt}$ response and restores ROS levels to those seen under nutrient-replete conditions. These results indicate that, while Pi availability does not seem to be signalled through $[Ca^{2+}]_{cyt}$, Pi starvation strongly affects stress-induced $[Ca^{2+}]_{cyt}$ signatures. The data reveal how plants can integrate nutritional and environmental cues, adding another layer of complexity to the use of Ca^{2+} as a signal transducer.

INTRODUCTION

Plant roots foraging in the soil have to sense, transduce, and respond to fluctuations in water and nutrients, plus a multitude of stresses they may additionally be subjected to. Plants employ a wide range of signal transducers, with free calcium ion (Ca^{2+}) being a common second messenger in the response to stress stimuli. Biotic and abiotic stresses (including mechanical, salt, osmotic, and oxidative stress) trigger rapid and transient modulations in cytosolic and organellar free Ca^{2+} (Knight et al., 1991, 1992, 1997; Kiegle, C. Moore, et al., 2000; Monshausen et al., 2009; Loro et al., 2012; Bonza et al., 2013; Laohavisit et al., 2013; Loro et al., 2016; Behera et al., 2018; Manishankar et al., 2018). These "Ca^{2+} signatures" are held to be specific to the stimulus and result in stimulus-specific outcomes, enabled by suites of decoding proteins (Whalley et al., 2011; Whalley and Knight, 2013; Liu et al., 2015; Lenzoni et al., 2017).

Recently, Ca^{2+} has been described as also functioning in signalling nutrient status and availability. In the model plant Arabidopsis (*Arabidopsis thaliana*), nitrate resupply to initially nitrate-starved roots prompted a rapid (within seconds) and monophasic increase in cytosolic free Ca^{2+} ($[Ca^{2+}]_{cyt}$), followed by an increase in nuclear $[Ca^{2+}]$ (Riveras et al., 2015; Liu et al., 2017). Potassium (K^+) deficiency was found to trigger two distinct $[Ca^{2+}]_{cyt}$ elevations within the Arabidopsis root, the first response occurring within 1 to 4 minutes, and the second response within 18 to 32 hours after onset of K^+ deficiency (Behera et al., 2017). $[Ca^{2+}]_{cyt}$ signalling was further found to be necessary for vacuolar magnesium (Mg^{2+}) detoxification in a high Mg^{2+} environment (Tang et al., 2015).

Another nutrient of great importance for optimal plant growth is inorganic phosphate (Pi). Pi-limited conditions are known to induce profound changes in plant growth and metabolism. On a systemic level, root growth is favored over shoot growth, indicative of maximizing soil exploration and, thus, nutrient uptake (Gruber et al., 2013). In addition, root system architecture is remodelled, which has been well described in many crop species, such as barley (*Hordeum vulgare*), maize (*Zea mays*), rice, (*Oryza sativa*) and tomato (*Solanum lycopersicum*), as well as Arabidopsis (Peret et al., 2014). Multicomponent nutrient studies found Pi to be the predominant nutrient controlling primary root length (Gruber et al., 2013; Kellermeier et al., 2014). On a cellular level, metabolism shifts to alternative pathways that consume less Pi (Pratt et al., 2009; Plaxton and Tran, 2011; Nakamura, 2013; Pant et al., 2015). The Pi deficiency response is orchestrated by intricate signalling networks, involving hormones, nutrient crosstalk, and transcriptional and translational feedback loops (reviewed by *e.g.* Abel, 2017; Chien et al., 2018). Ca^{2+} has been hypothesized to be involved as a signal transducer (Chiou and Lin, 2011; Linn et al., 2017; Chien et al., 2018), but this has not been confirmed to date.

While the involvement of Ca^{2+} as a second messenger in nutrient signalling is now beginning to be explored, few studies have examined the impact of nutrient deficiency on Ca^{2+} signalling per se. Boron-deprived tobacco BY-2 cells (expressing cytosolic aequorin as a luminometric reporter of $[Ca^{2+}]_{cyt}$) sustained an enhanced $[Ca^{2+}]_{cyt}$ signature when challenged with 3 mM Ca^{2+} compared to boron-replete cells (Koshiba et al., 2010). Boron deficiency caused an increase in steady-state $[Ca^{2+}]_{cyt}$ of Arabidopsis roots, but the consequences for stress-induced Ca^{2+} signatures were not examined (Quiles-Pando et al., 2013).

Thus, we set out to test how Pi starvation of Arabidopsis might influence the root's use of Ca^{2+} as a signal, employing a range of abiotic stresses known to evoke robust, rapid, and transient $[Ca^{2+}]_{cyt}$ signatures (mechanical, salt, osmotic, and oxidative stress). Additionally, as mechanical stimulation, salt, and osmotic stress increase the accumulation of extracellular adenosine 5'-triphosphate (eATP; Weerasinghe et al., 2009; Dark et al., 2011), which in turn transiently increases $[Ca^{2+}]_{cyt}$ (Demidchik

et al., 2003; Tanaka et al., 2010; Costa et al., 2013; Choi et al., 2014), we also tested the root response to extracellular purine nucleotides.

We show that Pi starvation, but not nitrogen (N) starvation, strongly altered $[Ca^{2+}]_{cyt}$ signatures in response to all abiotic stresses and extracellular nucleotides tested. Furthermore, Pi-starved root apices of Arabidopsis showed a distinct spatiotemporal $[Ca^{2+}]_{cyt}$ response to eATP. This was remodelled during development and was dependent on iron (Fe) availability and reactive oxygen species (ROS) production but could be reversed by Pi resupply. The data reveal how nutritional status adds another so far unexplored level of complexity to the use of $[Ca^{2+}]_{cyt}$ as a signal transducer and further our understanding of how plants integrate various environmental cues.

110

RESULTS

Pi, but not N, starvation dampens the $[Ca^{2+}]_{cyt}$ response to abiotic stresses in Arabidopsis root tips

To determine if Pi starvation alters stress-induced $[Ca^{2+}]_{cyt}$ signatures, Arabidopsis seedlings ubiquitously expressing cytosolic (apo)aequorin were grown on Pi-replete conditions (0.625 mM KH_2PO_4, "full Pi"), lowered Pi conditions (0.1 mM KH_2PO_4, "medium Pi"), or chronically starved of Pi (0 mM KH_2PO_4, "zero Pi"). As has been reported previously (Williamson et al., 2001; Svistoonoff et al., 2007; Balzergue et al., 2017), Pi starvation for 10 days led to significantly shorter primary roots (mean root length ± standard error of means; full Pi: 6.01 ± 0.06 cm; medium Pi: 4.42 ± 0.04 cm; zero Pi: 2.69 ± 0.04 cm, *p*-value < 0.001 for all comparisons; Supplemental Table S1). To account for differences in root growth and architecture induced by Pi growth regime, a fixed length of the primary root (the first 1 cm from the apex) from an 11-day-old seedling was challenged with acute abiotic stress and aequorin luminescence was recorded every second for 155 seconds (Fig. 1). As the experimental setup necessitates the injection of treatment solutions, control solution treatments were run with every set of experiments to control for the effect of mechanical stimulation.

An immediate and monophasic increase in $[Ca^{2+}]_{cyt}$ was observed upon mechanical stimulation (application of control solution, Fig. 1A-C), salt stress (150 mM NaCl, Fig. 1D-F), or an equivalent osmotic stress (280 mM D-sorbitol, Fig. 1G-I). The response to mechanical stimulation was variable in root tips of all Pi growth conditions, likely due to limitations of the experimental setup, but overall, the Pi-starved root tip response was significantly lower. The response to salt and osmotic stress was as immediate as the response to mechanical stimulation, but of much greater amplitude and duration in root tips from all Pi growth conditions. In all cases, Pi starvation significantly dampened the stress-induced $[Ca^{2+}]_{cyt}$ response (as quantified by peak maxima (Fig. 1B, E, H) and area under the curve (as a proxy of how much $[Ca^{2+}]_{cyt}$ was mobilized upon stress treatment; Fig. 1C, F, I, see Supplemental Fig. S1 for details). For all stress experiments, Pi-replete root tips showed the strongest $[Ca^{2+}]_{cyt}$ response, medium Pi root tips showed a moderately dampened $[Ca^{2+}]_{cyt}$ response, and Pi-starved root tips showed the most strongly impaired $[Ca^{2+}]_{cyt}$ response.

To test if this dampened $[Ca^{2+}]_{cyt}$ response were specific to Pi nutrition or due to a more general nutrient deficiency response, we trialled root tips starved of another macronutrient, nitrogen (N). Primary root lengths of severely N-starved plants (0 mM N) were comparable to zero-Pi-grown roots (zero N: 2.5 ± 0.13 cm, $p = 0.203$, Supplemental Table S1). However, N-starved root tips showed a $[Ca^{2+}]_{cyt}$ response to mechanical stimulation, salt, and osmotic stress, which was similar to nutrient-replete root tips (Supplemental Fig. S2). These results indicate that Pi nutrition specifically alters the $[Ca^{2+}]_{cyt}$ response to abiotic stresses.

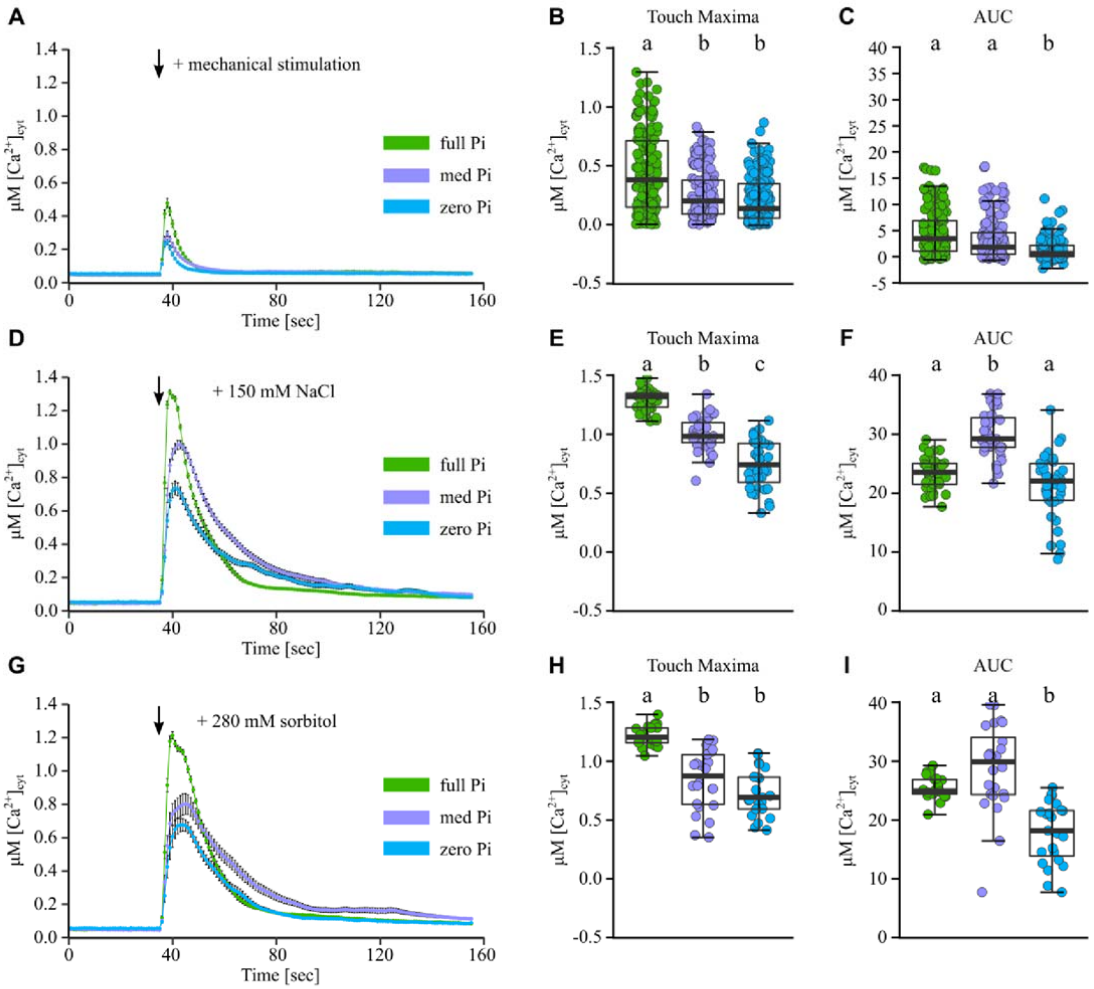

Figure 1. Pi-starved root tips have a dampened $[Ca^{2+}]_{cyt}$ response to mechanical, salt and osmotic stress. Arabidopsis Col-0 aequorin-expressing seedlings were grown on full, medium (med) or zero Pi (green, purple, blue trace respectively). Individual root tips (1 cm) of 11-day old seedlings were challenged with treatments applied at 35 seconds (black arrow), and $[Ca^{2+}]_{cyt}$ was measured for 155 seconds. (A) Mechanical stimulation (control solution); time course trace represents mean ± standard error of mean (SEM) from 18 independent trials, with n = 150 - 155 root tips per growth condition averaged per data point. Time course data were analysed for (B) Touch Maxima and (C) area under the response curve (AUC), both baseline-subtracted, with each dot representing an individual data point (see Supplemental Fig. S1 for analysis details). Boxplot middle line denotes median. (D-F) Responses to 150 mM NaCl (3 independent trials, n = 35 – 36 root tips). (G-I) Responses to 280 mM sorbitol (3 independent trials, n = 22 - 24 root tips). Analysis of variance (ANOVA) with *post-hoc* Tukey Test was used to assess statistical differences, different lower-case letters denote significant differences ($p < 0.05$).

Pi starvation alters the root tip $[Ca^{2+}]_{cyt}$ response to extracellular nucleotides and ROS

Mechanical stimulation, salt, and osmotic stress are known to evoke the accumulation of extracellular ATP (eATP), which in turn triggers increases in ROS (Kim et al., 2006; Song et al., 2006; Demidchik et al., 2009, 2011; Chen et al., 2017), and ROS such as hydrogen peroxide (H_2O_2) induce $[Ca^{2+}]_{cyt}$ increases (Price et al., 1994; Rentel and Knight, 2004; Demidchik et al., 2007; Richards et al., 2014). Therefore, we next challenged aequorin-expressing root tips from 11-day-old seedlings, grown on full/medium/zero Pi conditions, with 0.1 or 1 mM eATP. eATP treatment evoked robust multiphasic $[Ca^{2+}]_{cyt}$ increases in full Pi-grown root tips (Fig. 2), as reported previously (Demidchik et

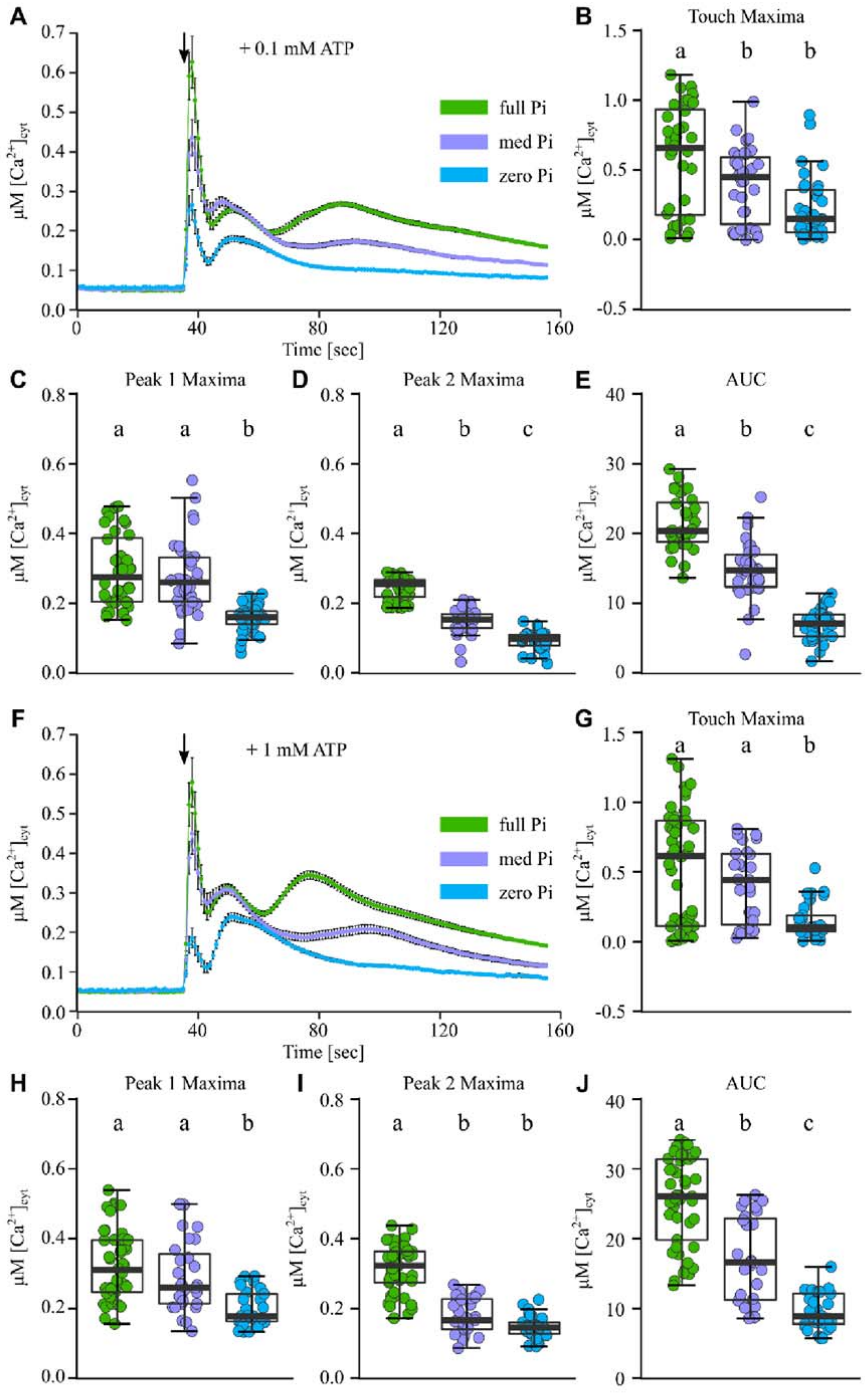

Figure 2. Pi-starved root tips show a dampened $[Ca^{2+}]_{cyt}$ response to extracellular ATP. Arabidopsis Col-0 aequorin-expressing seedlings were grown on full, medium (med) or zero Pi (green, purple, blue trace respectively). Individual root tips (1 cm) of 11-day old seedlings were challenged with treatments applied at 35 seconds (black arrow), and $[Ca^{2+}]_{cyt}$ was measured for 155 seconds. (A) Treatment with 0.1 mM ATP; time course trace represents mean ± standard error of mean (SEM) from 6 independent trials, with n = 34 - 36 individual root tips averaged per data point. Time course data were analysed for (B) Touch Maxima, (C) Peak 1 Maxima and (D) Peak 2 Maxima, (E) area under the response curve (AUC), all baseline-subtracted, with each dot representing an individual data point (see Supplementary Fig. S1 for analysis details). Boxplot middle line denotes median. (F-J) Responses to 1 mM ATP (5 independent trials, n = 27 - 45 root tips per growth condition). Analysis of variance (ANOVA) with *post-hoc* Tukey Test was used to assess statistical differences, different lower-case letters denote significant differences ($p < 0.05$).

al., 2003; Tanaka et al., 2010). The different phases of the response were classified as an immediate 'touch response' (0 – 6 seconds after treatment application), followed by 'peak 1' (7 – 28 seconds after treatment application) and subsequent 'peak 2' (29 – 120 seconds after treatment application, see Supplemental Fig. S1 for details). The touch response elicited by eATP was variable but overall

not significantly different to application of control solution alone (see Fig. 1A) and was nonresponsive to an increase in eATP concentration (Fig. 2B: 0.1 mM eATP, Fig. 2G: 1 mM eATP), indicating that this initial response was due to mechanical stimulation of treatment application rather than eATP perception.

In contrast, the subsequent $[Ca^{2+}]_{cyt}$ increases (defined as peak 1 and peak 2) were specific to eATP treatment, and their magnitude was dependent on root Pi status. Peak 1 maxima were similar between full Pi- and medium Pi-grown root tips but significantly dampened in zero-Pi-grown root tips in response to 0.1 mM ATP (Fig. 2C) and 1 mM ATP (Fig. 2H). Peak 2 maxima were significantly dampened in medium Pi root tips compared to full Pi root tips, with zero Pi root tips mostly lacking any apparent $[Ca^{2+}]_{cyt}$ increase within that phase (Fig. 2D, I). Overall, the more Pi-starved the roots, the less $[Ca^{2+}]_{cyt}$ was mobilized in response to eATP (based on the area under the response curves, Fig. 2E, J). While increasing the eATP concentration 10-fold (from 0.1 mM to 1 mM eATP) significantly increased the $[Ca^{2+}]_{cyt}$ mobilized of full Pi root tips, medium and zero Pi root tips were insensitive to an increase in eATP concentration.

As up to 2 mM Pi could potentially be liberated readily from 1 mM eATP, and this Pi pulse itself might evoke a $[Ca^{2+}]_{cyt}$ response, we treated root tips with a Pi source alone. Application of 2 mM Pi led to a rapid and monophasic increase in $[Ca^{2+}]_{cyt}$, very similar in shape, duration, and amplitude to control solution treatment across all three Pi growth regimes (Supplemental Fig. S3). This indicated that under the Pi starvation conditions tested, Pi alone did not trigger an increase in $[Ca^{2+}]_{cyt}$, in contrast to what had been reported for nitrate resupply in a similar setup (Riveras et al., 2015). To further test if ATP hydrolysis played a role in the differing $[Ca^{2+}]_{cyt}$ signatures, adenosine 5'-diphosphate (ADP) and a nonhydrolyzable ATP analog (adenosine 5'-[γ-thio]triphosphate tetralithium, γ-ATP) were applied to root tips from the different Pi growth regimes. ADP and γ-ATP treatment (1 mM) resulted in $[Ca^{2+}]_{cyt}$ signatures strikingly similar to those observed with 1 mM eATP treatment (Supplemental Fig. S4 and S5), indicating that ATP hydrolysis could not mechanistically explain the altered $[Ca^{2+}]_{cyt}$ signature of Pi-starved roots.

Next, we applied ROS, as 1 and 5 mM H_2O_2, to excised root tips. This treatment induced a rapid increase in $[Ca^{2+}]_{cyt}$ followed by a pronounced secondary increase (Supplemental Fig. S6). Full-Pi- and medium-Pi-grown root tips showed a similar $[Ca^{2+}]_{cyt}$ response, while zero-Pi-grown root apices showed a significantly dampened secondary response to both H_2O_2 concentrations tested (Supplemental Fig. S6). N-starved root apices did not show a dampened response to either 1 mM eATP (Supplemental Fig. S7) or 1 mM H_2O_2 (Supplemental Fig. S8), again indicating that the severely altered $[Ca^{2+}]_{cyt}$ signature observed in Pi-starved roots was not a general response to nutrient starvation, but a consequence specific to Pi nutrition.

Pi-starved roots respond to eATP at the root apex, but a secondary $[Ca^{2+}]_{cyt}$ response in the distal region is lost

As the aequorin-based $[Ca^{2+}]_{cyt}$ determinations did not allow spatial resolution, we employed ratiometric imaging to map the $[Ca^{2+}]_{cyt}$ response of the root. Arabidopsis Col-0 constitutively expressing the ratiometric $[Ca^{2+}]_{cyt}$ reporter Yellow Cameleon YC3.6 (NES-YC3.6, Krebs et al., 2012) was grown on full Pi or zero Pi, and intact 10-day-old plants were mounted into a custom-built perfusion chamber (Behera and Kudla, 2013) with shoots exposed to air and roots constantly superfused with control imaging solution. This constant superfusion system circumvented mechanical stimulation due to treatment injection (present in aequorin-based assays), excluding any 'touch response.' As eATP application had so far produced the most prominent Pi-dependent

$[Ca^{2+}]_{cyt}$ response and was at the crossroads of signalling in other stress pathways, we used it as the standard treatment from here onwards.

In Pi-replete roots of NES-YC3.6-expressing seedlings (Fig. 3A), superfusion with 1 mM eATP led to a strong increase in cpVenus/CFP ratio over prestimulus levels in the apex (approximately within the first 1 mm), which was sustained over the period of eATP treatment (3 minutes, visualized as a representative kymograph in Fig. 3B). Approximately 30 to 40 seconds after this initial response, a secondary increase in ratio occurred in the more distal part of the root tip (≥ 1 mm from root apex), which appeared to propagate along the root (Fig. 3B, Supplemental Movie S1). These two distinct increases in $[Ca^{2+}]_{cyt}$ were reminiscent of what had been termed 'peak 1' and 'peak 2' in aequorin-based assays (see Fig. 2).

Pi-starved roots (Fig. 3C) sustained a similar increase of cpVenus/CFP ratio at the root apex in response to 1 mM eATP. In more distal parts of the roots (≥ 1 mm from root apex), Pi-starved roots only showed a slight or no ratio increase at all in response to eATP treatment (Fig. 3D: representative kymograph, Supplemental Movie S2). This lack of a secondary response resembled the absence of peak 2 in Pi-starved aequorin-expressing root tips (Fig. 2). Quantifying the ratiometric changes occurring in response to eATP in specific regions of interest (ROIs) along the root (apical 2.5 mm, see micrograph in Fig. 4) corroborated these observations. Pi starvation effectively abolished an eATP-induced $[Ca^{2+}]_{cyt}$ elevation in more distal regions (Fig. 4A-D) and dampened it nearer to the apex (Fig. 4 E,F). However, at the apex, Pi starvation had no effect on the eATP-induced $[Ca^{2+}]_{cyt}$ elevation (Fig. 4 G,H; n = 7 -9 roots per growth condition), indicating that Pi-starved roots were not impaired in perceiving eATP per se.

The altered $[Ca^{2+}]_{cyt}$ signature manifests during prolonged Pi starvation and is reversed by Pi resupply

To place the response of Pi-starved root tips into developmental context, we next tested aequorin-expressing Arabidopsis of different ages for an altered $[Ca^{2+}]_{cyt}$ response to eATP. The youngest root material tested (on day 6) did not yet significantly differ in primary root length between full-Pi- and zero-Pi-grown plants (mean primary root length ± SEM: full Pi: 1.99 ± 0.08 cm, zero Pi: 1.83 ± 0.04 cm, p = 0.908). In ≥7-day-old material, a significantly shorter primary root was observed in Pi-starved seedlings (also see Supplementary Table S1).

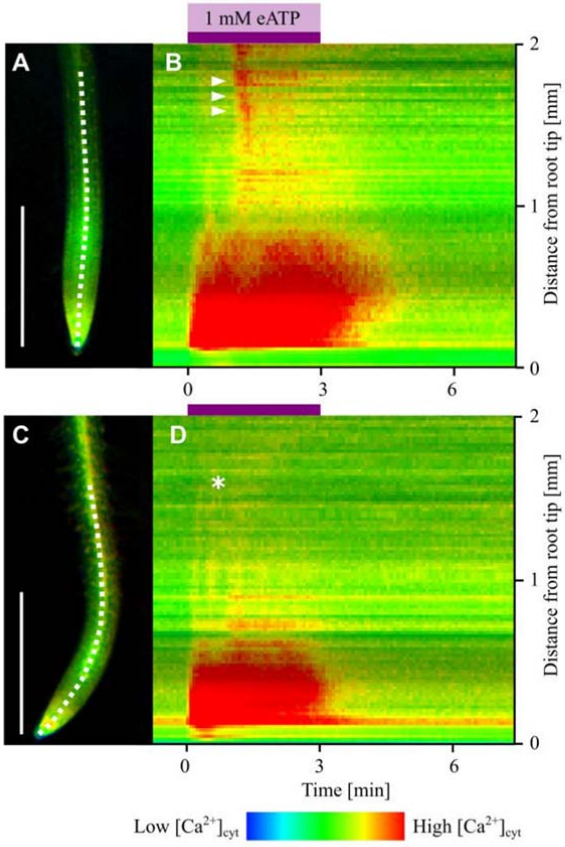

Figure 3. Extracellular ATP elicits two spatiotemporally distinct $[Ca^{2+}]_{cyt}$ increases in the root, which are altered by Pi starvation. (A) Representative full Pi-grown Arabidopsis Col-0 root expressing NES-YC3.6, white dashed line in root micrograph indicates line used for kymograph extraction, scale bar: 1 mm. (B) Kymograph depicts temporal and spatial changes in $[Ca^{2+}]_{cyt}$ of a representative full Pi-grown root in response to a 3-minute 1 mM eATP treatment (purple bar), preceded and followed by superfusion with control imaging solution. (C, D) Representative zero Pi-grown root. White triangles indicate secondary increase in $[Ca^{2+}]_{cyt}$ in the full Pi root, which is missing in the zero Pi root (marked by white star).

Assaying 6-, 7-, 8-, and 11-day-old full Pi-grown root tips (1 cm) replicated the characteristic multiphasic $[Ca^{2+}]_{cyt}$ response to 1 mM eATP throughout development (Fig. 5A-D), as well as eliciting $[Ca^{2+}]_{cyt}$ responses of comparable magnitude (quantified as area under the response curves, Fig. 5E). In contrast, 6-day-old Pi-starved root tips showed a $[Ca^{2+}]_{cyt}$ response comparable in shape to the response of Pi-replete tips, but was dampened in magnitude (Fig. 5A). Seven- and 8-day-old Pi-starved tips (1 cm) showed a much dampened peak 2, which was completely absent in 11-day-old tips (Fig. 5B-D). Concomitantly, Pi-starved tips showed a decrease in total mobilized $[Ca^{2+}]_{cyt}$ with prolonged growth on zero Pi medium (Fig. 5E).

To test if the dampened and altered $[Ca^{2+}]_{cyt}$ response of Pi-starved root tips could be rescued by Pi resupply, or was irreversibly lost, we grew seedlings on zero Pi medium until the altered $[Ca^{2+}]_{cyt}$ response to eATP would have manifested (day 8). On day 8, seedlings were (i) not transferred, (ii) transferred to zero Pi growth medium (representing a transfer control), or (iii) transferred to full Pi growth medium and grown for another 2 days. Pi-starved root tips (both not transferred and transferred to zero Pi) showed a dampened $[Ca^{2+}]_{cyt}$ response to 1 mM eATP, with peak 2 being mostly absent. In contrast, seedlings that had been resupplied with Pi (zero Pi to full Pi transfer) showed a clear multiphasic $[Ca^{2+}]_{cyt}$ response to eATP (Fig. 6A). Resupply of Pi significantly rescued the amplitude of peak 1 and peak 2, as well as the overall response magnitude (Fig. 6C-E).

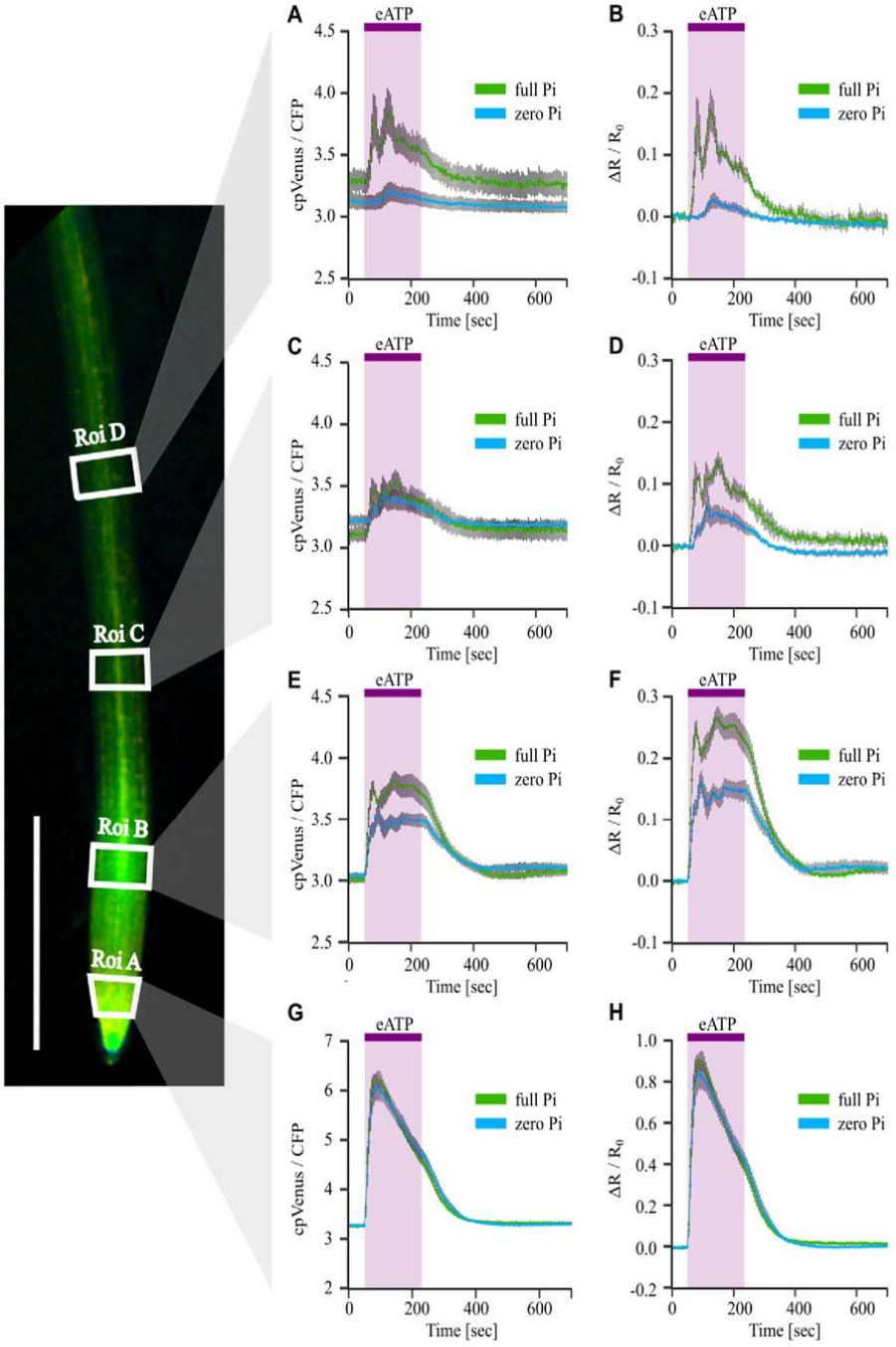

Figure 4. Quantification of differential $[Ca^{2+}]_{cyt}$ response of Pi-starved roots to eATP. Arabidopsis Col-0 expressing the cytosolic Yellow Cameleon 3.6 (NES-YC3.6) was grown on full or zero Pi. In a superfusion chamber, a root of a 10-day old seedling was superfused with imaging solution before switching to 1 mM eATP (applied during 50 – 230 second interval after start of image acquisition, purple shading), followed by wash-out with imaging solution. On the left, representative root with annotated regions of interest ("Roi", white boxes), analysed and plotted over time in A – H, scale bar: 1 mm. (A, B): Roi D; (C, D): Roi C; (E, F): Roi B; (G, H): Roi A. (A, C, E, G) Mean FRET ratio (cpVenus/CFP) ± SEM, background subtracted; (B, D, F, H) normalized FRET ratio ($\Delta R/R_0$) ± SEM, of full Pi (green trace) and zero Pi roots (blue trace). Data from 3 independent trials, with n = 7 - 9 individual roots per growth condition.

263 **Iron exclusion restores the eATP-induced $[Ca^{2+}]_{cyt}$ signature in Pi-starved root tips**

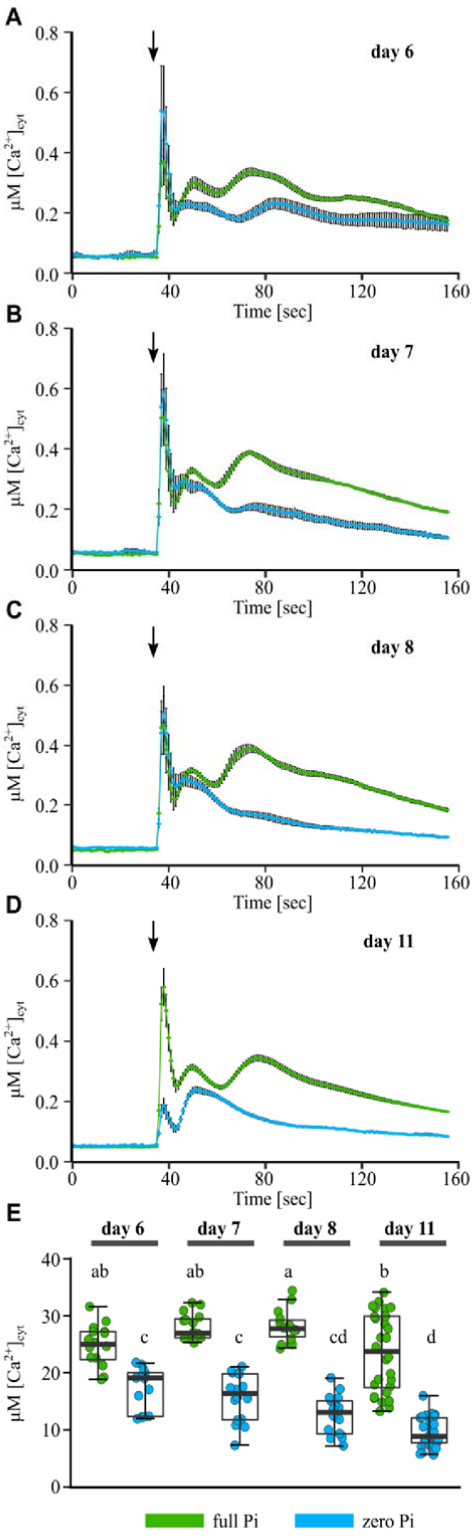

Figure 5. Pi starvation modulates the root tip $[Ca^{2+}]_{cyt}$ response to eATP during development. Arabidopsis Col-0 aequorin-expressing seedlings were grown on full or zero Pi (green, blue trace respectively). Root tips (1 cm) of (A) 6-day, (B) 7-day, (C) 8-day or (D) 11-day old seedlings were challenged with 1 mM eATP applied at 35 seconds (black arrow), and $[Ca^{2+}]_{cyt}$ was measured for 155 seconds. Time course trace represents mean ± standard error of mean (SEM) from 3 - 5 independent trials, with n = 13 - 45 individual root tips averaged per data point. Time course data were analysed for (E) area under the curve (AUC), baseline-subtracted, with each dot representing an individual data point, see Supplemental Fig. S1 for analysis details. Boxplot middle line in (E) denotes median. Analysis of variance (ANOVA) with *post-hoc* Tukey Test was used to assess statistical differences. Different lower-case letters describe groups of significant statistical difference ($p < 0.05$), same letters indicate no statistical significance ($p > 0.05$).

Pi starvation causes iron (Fe) accumulation in Arabidopsis root tips, and exclusion of Fe from the growth medium (as well as Pi) restores primary root growth (Svistoonoff et al., 2007; Ward et al., 2008; Ticconi et al., 2009; Müller et al., 2015; Balzergue et al., 2017). To test if Fe availability

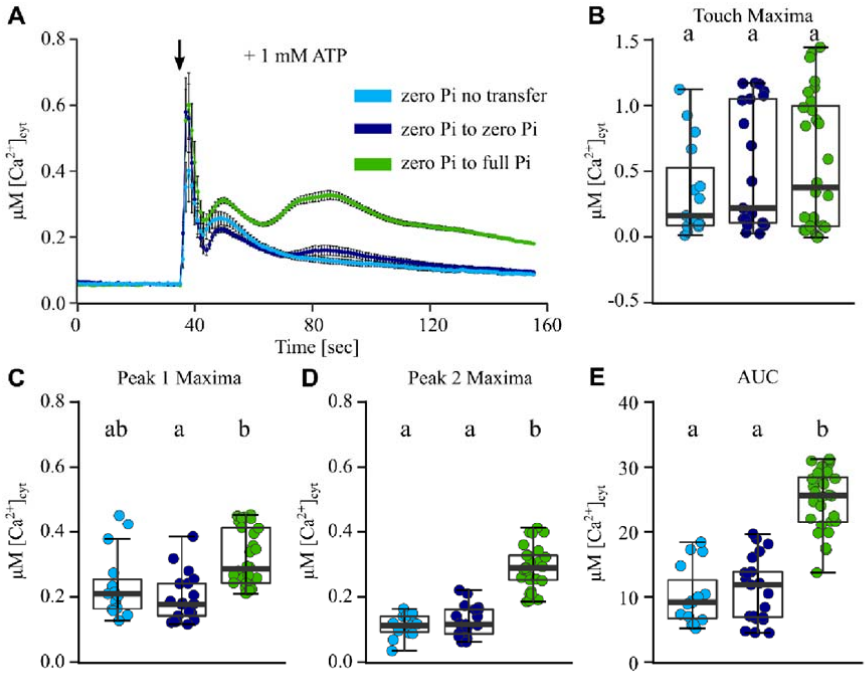

Figure 6. Resupply of Pi to Pi-starved seedlings rescues the dampened root tip $[Ca^{2+}]_{cyt}$ response to eATP. Arabidopsis Col-0 expressing aequorin was grown on zero Pi for 8 days, when plants were (i) not transferred ('zero Pi no transfer'), (ii) transferred to zero Pi growth medium ('zero Pi to zero Pi'), or (iii) transferred to full Pi growth medium ('zero Pi to full Pi'). After 2 days, individual excised root tips (1 cm) were challenged with treatments applied at 35 seconds (black arrow), and $[Ca^{2+}]_{cyt}$ was measured for 155 seconds. (A) Application of 1 mM ATP; time course trace represents mean ± standard error of mean (SEM) from 3 independent trials, with n = 15 - 28 individual root tips averaged per data point. Time course data were analysed for (B) Touch Maxima, (C) Peak 1 Maxima, (D) Peak 2 Maxima and (E) area under the response curve (AUC), all baseline-subtracted, with each dot representing an individual data point (see Supplementary Fig. S1 for analysis details). Boxplot middle line denotes median. Analysis of variance (ANOVA) with *post-hoc* Tukey Test was used to assess statistical differences, different lower-case letters describe significant differences ($p < 0.05$).

influences the Pi starvation effect on the eATP-induced $[Ca^{2+}]_{cyt}$ signature, we again grew aequorin-expressing plants on varied Pi levels (full Pi: 0.625 mM Pi, zero Pi: 0 mM Pi) while additionally varying Fe levels (full Fe: 50 µM Fe, low Fe: 10 µM, zero Fe: 0 µM Fe). As expected, Fe exclusion in a zero Pi background rescued primary root growth (Supplementary Table S1). Strikingly, this growth condition (zero Pi-zero Fe) also rescued the altered root tip $[Ca^{2+}]_{cyt}$ response to 1 mM eATP induced by Pi starvation alone (zero Pi-full Fe; Fig. 7A). Zero Pi-zero Fe-grown roots supported an eATP-induced $[Ca^{2+}]_{cyt}$ signature similar to those grown in nutrient-replete (full Pi-full Fe) conditions (Fig. 7B-E).

An intermediate Fe level in a Pi-deplete background (zero Pi-low Fe) led to an intermediate $[Ca^{2+}]_{cyt}$ response to 1 mM eATP for all parameters quantified (touch response: Fig. 7B, peak 1 maxima: Fig. 7C, peak 2 maxima: Fig. 7D, area under the response curve: Fig. 7E). This was particularly interesting as zero Pi-low Fe-grown plants had longer root lengths than full Pi-full Fe-grown plants (Supplementary Table S1), indicating that long primary roots alone could not explain the rescued, altered $[Ca^{2+}]_{cyt}$ signature. As a test of Fe specificity, copper (Cu^{2+}; also a micronutrient transition metal) was excluded from the zero Pi growth medium. This treatment rescued neither primary root growth nor the eATP-induced $[Ca^{2+}]_{cyt}$ signature (Supplementary Table S1; Supplemental Fig. S9).

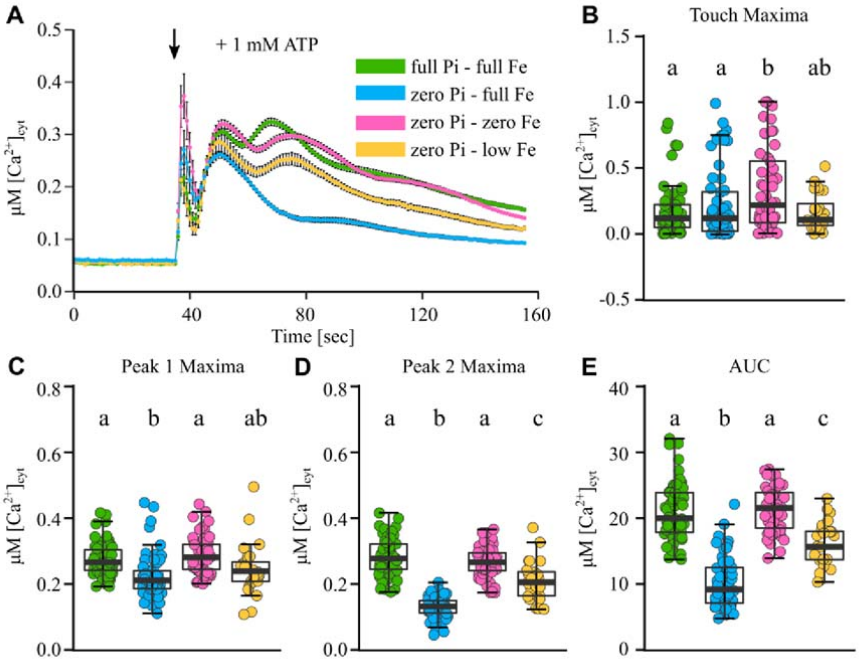

Figure 7. Iron levels modify the $[Ca^{2+}]_{cyt}$ response of Pi-starved root apices to eATP. Arabidopsis Col-0 aequorin-expressing seedlings were grown on standard half MS growth medium, full Pi-full Fe (green trace), zero Pi-full Fe (blue trace), zero Pi-low Fe (pink trace) or zero Pi-zero Fe (orange trace). Excised root apices (1 cm) of 11-day old seedlings were challenged with treatments applied at 35 seconds (black arrow), and $[Ca^{2+}]_{cyt}$ was measured for 155 seconds. (A) Application of 1 mM eATP; time course trace represents mean ± standard error of mean (SEM) from 3 - 6 independent trials, with n = 24 - 61 individual root tips averaged per data point. Time course data were analysed for (B) Touch Maxima, (C) Peak 1 Maxima, (D) Peak 2 Maxima, and (E) area under the response curve (AUC), all baseline-subtracted, with each dot representing an individual data point (see Supplemental Fig. S1 for details). Boxplot middle line denotes median. Analysis of variance (ANOVA) with *post-hoc* Tukey Test was used to assess statistical differences, different lower-case letters describe significant differences ($p < 0.05$).

Pi and Fe availability influences root cellular ROS level

Pi-dependent Fe accumulation has been linked to hotspots of ROS (Müller et al., 2015; Balzergue et al., 2017), implying a link between cellular redox status and aberrant $[Ca^{2+}]_{cyt}$ response to eATP of Pi-starved root tips. Using the fluorescent dye CM-H_2DCFDA (which reports intracellular ROS), nutrient-replete roots showed low intracellular ROS levels along the root tip (Fig. 8A,B). In Pi-starved root tips, we observed overall higher ROS levels, with a particular ROS hotspot localized at approximately 1 mm from the root apex (Fig. 8C, D, also see blue trace in I). Excluding Fe (in zero Pi background) reversed the higher ROS load back to nutrient-replete low ROS levels (Fig. 8E, F). Thus, root tips sustaining a low ROS load qualitatively correlated with root tips capable of producing a multiphasic $[Ca^{2+}]_{cyt}$ response to 1 mM eATP (compare with Fig. 7). Root tips showing a high ROS load correlated with root tips exhibiting a much dampened $[Ca^{2+}]_{cyt}$ response to 1 mM eATP.

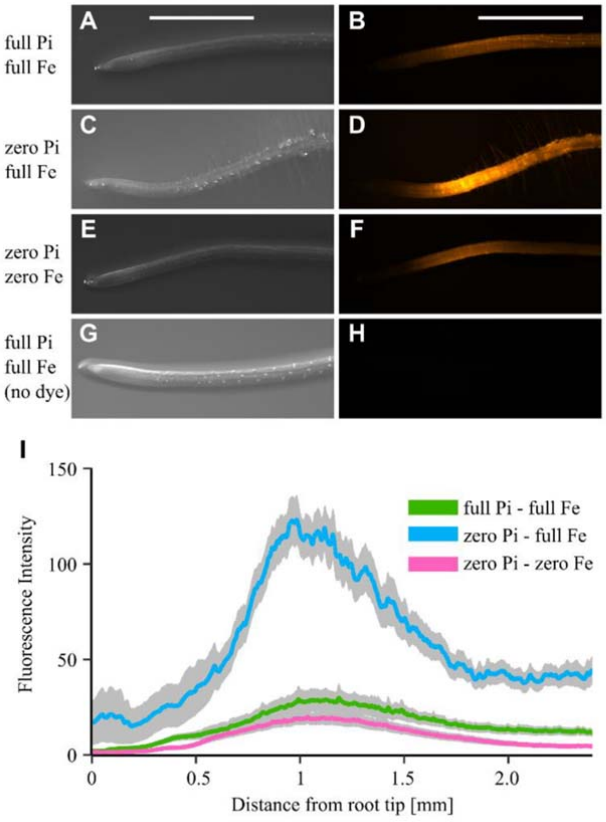

Figure 8. Intracellular ROS are modified by Pi and Fe availability, and influence root $[Ca^{2+}]_{cyt}$ response to eATP. Ten- to 11-day old Arabidopsis Col-0 grown on (A,B) full Pi-full Fe, (C,D) zero Pi-full Fe, (E,F) zero Pi-zero Fe were stained for intracellular ROS using 20 µM CM-H_2DCFDA, (G,H) non-stained control root, (A,C,E,G) representative brightfield images, (B,D,F,H) representative false-coloured fluorescence images, scale bar in (A,B) 1 mm. (I) Fluorescence intensity was quantified, background subtracted and averaged along the root length. Mean values (coloured lines) ± SEM (grey shading) are shown, data from 3 independent trials, with n = 14 - 16 roots analysed per growth condition.

296

297

298

DISCUSSION

$[Ca^{2+}]_{cyt}$ is a seemingly ubiquitous second messenger in plant abiotic stress responses, with roots responding to such stresses with cell-specific Ca^{2+} signatures (Kiegle et al., 2000; Marti et al., 2013; Wilkins et al., 2016). Few studies have addressed the impact of nutrient status on Ca^{2+} signatures (Koshiba et al., 2010; Quiles-Pando et al., 2013). Here, we show that Pi but not N starvation could significantly affect the root tip $[Ca^{2+}]_{cyt}$ response to a range of acute abiotic stressors and intermediate signalling agents (extracellular purine nucleotides and H_2O_2). Pi and Ca^{2+} have a particularly interesting relationship as they can form undissociated complexes (Cole, 1953; Edel and Kudla, 2015; Verkhratsky and Parpura, 2015). In animals, Ca^{2+}-Pi complexes play significant structural roles (Plattner and Verkhratsky, 2015), but in plants, these have only recently been discovered in trichomes of a variety of plant species, including Arabidopsis (Ensikat et al., 2016; Weigend et al., 2017; Mustafa et al., 2018). Pi and Ca^{2+} have even been shown to be stored in different plant cell types, presumably to avoid complexation (Conn and Gilliham, 2010). Cellular Pi levels have favored the evolution of a highly efficient and regulated Ca^{2+} flux apparatus to maintain low $[Ca^{2+}]_{cyt}$ and prevent cytotoxicity (Edel and Kudla, 2015; Verkhratsky and Parpura, 2015). While Pi deficiency causes lower cellular and cytosolic Pi levels (Duff et al., 1989; Pratt et al., 2009), results here show that $[Ca^{2+}]_{cyt}$ signatures still proceed but in altered forms.

The impact of Pi depletion on the eATP-induced $[Ca^{2+}]_{cyt}$ signature was evident in 6-day-old root tips, at a stage where a Pi-dependent inhibition of primary root growth was not yet detectable. This suggests that changes in Ca^{2+} transport and possibly signalling systems are an early consequence of Pi deprivation. The observed dampening of $[Ca^{2+}]_{cyt}$ signatures under Pi deprivation may have several causes. Pi deficiency causes remodelling of membranes such that phospholipids are replaced by glyco- and sulpholipids (Andersson et al., 2005; Tjellstrom et al., 2010; Nakamura, 2013; Okazaki et al., 2013), which can be envisaged to have an impact on membrane-based signalling. Additionally, many studies have reported the effect of Pi starvation on gene expression and protein composition (Misson et al., 2005; Lin et al., 2011; Lan et al., 2012; Kellermeier et al., 2014; Hoehenwarter et al., 2016; Wang et al., 2018). However, these studies do not report an enrichment of (downregulated) Ca^{2+}-associated transport and signalling components to help explain dampening of the $[Ca^{2+}]_{cyt}$ signature. As phosphorylated metabolites decrease, and phosphorylation patterns reportedly change under Pi starvation (Duan et al., 2013; Pant et al., 2015), it could be envisaged that posttranslational modifications and an altered physico-chemical cellular environment strongly affect the activity of the channels involved in generating the signatures.

Therefore, it is likely that as Pi starvation advances there is a progressive remodelling of Ca^{2+} signalling machinery, affecting the transporters engaged in generating $[Ca^{2+}]_{cyt}$ signatures. Our results show that this is not a determinate effect, but reversible by Pi resupply. These findings have implications for the downstream signalling events and responses, which may change under Pi deprivation. For example, Pi deprivation dampened the mechano-induced $[Ca^{2+}]_{cyt}$ signature, which may have consequences for root penetration of Pi-deplete compacted soil. It also dampened the NaCl-induced $[Ca^{2+}]_{cyt}$ signature, which may have consequences for regulation of the Ca^{2+}-dependent SOS pathway (Quintero et al., 2011; Manishankar et al., 2018) and the observation that Pi starvation alleviated the inhibitory effect of low salt concentrations on root growth (Kawa et al., 2016).

The extracellular purine nucleotides ATP and ADP induce root $[Ca^{2+}]_{cyt}$ increases, potentially for regulation of growth, stress responses, and defense (Demidchik et al., 2003, 2009; Rincón-Zachary et al., 2010; Tanaka, Gilroy, et al., 2010; Dark et al., 2011; Loro et al., 2012, 2016; Choi et al., 2014). In common with root $[Ca^{2+}]_{cyt}$ imaging reports (Loro et al., 2012, 2016; Waadt et al., 2017), eATP was used here as a reliable stimulus of a robust $[Ca^{2+}]_{cyt}$ signature as well as an agent of root signal

transduction. Under Pi-replete conditions, the temporal biphasic eATP-induced $[Ca^{2+}]_{cyt}$ response found using aequorin mapped well to a spatial biphasic response found using YC3.6, as well as agreeing with what has recently been reported using a range of other $[Ca^{2+}]_{cyt}$ reporters (Waadt et al., 2017). This spatiotemporal pattern has been hypothesized to constitute a "Ca^{2+} wave," propagating from the meristematic zone towards the elongation zone and into the mature zone (Rincón-Zachary et al., 2010; Loro et al., 2012; Costa et al., 2013).

The spatial resolution afforded by YC3.6 revealed that while Pi starvation had no effect on the eATP-induced $[Ca^{2+}]_{cyt}$ increase at the apex (Fig. 4G,H), it caused the progressive diminution of the signal in increasingly distal regions in the mature zone (Fig. 4A-F). Root accumulation of intracellular ROS under Pi deficiency was linked to Fe availability (Fig. 8), consistent with previous reports (Müller et al., 2015; Balzergue et al., 2017). Fe depletion under Pi starvation not only lowered ROS accumulation to that found under nutrient-replete conditions but also restored the second peak of the biphasic eATP- induced $[Ca^{2+}]_{cyt}$ signature (with good spatial coincidence of both phenomena). It is therefore reasonable to conclude that under Pi deprivation alone, aberrant Fe accumulation leads to intracellular ROS accumulation and that the greater oxidative state of that region helps suppress the second eATP-induced $[Ca^{2+}]_{cyt}$ increase. Abiotic stress has been shown previously to cause an increase in root ROS accumulation, with NADPH oxidases implicated in their generation (Foreman et al., 2003; Demidchik et al., 2009). However, the activity of NADPH oxidases is usually linked to amplification of a $[Ca^{2+}]_{cyt}$ increase through activation of Ca^{2+} influx across the plasma membrane (Foreman et al., 2003; Demidchik et al., 2009; Laohavisit et al., 2012; Demidchik, 2018). This is seemingly at odds with the loss of the second eATP-induced $[Ca^{2+}]_{cyt}$ increase under Pi starvation, and the paradigm of the "ROS/Ca^{2+} hub" in signalling may not hold under Pi deprivation or in general conditions of high baseline ROS. The origin of the intracellular ROS under Pi deprivation may well include leakage from mitochondria, which increase their ROS production under stress (Gleason et al., 2011). It is feasible that the restoration of normal ROS levels with growth on zero Pi and zero Fe medium reflects the impaired mitochondrial function that occurs on chronic deprivation of Fe (Vigani and Briat, 2016), possibly leading to lower ROS production.

Overall, our results reveal how nutritional status adds another layer of complexity to Ca^{2+} signalling, allowing plants to integrate various cues such as nutritional status and environmental changes. While $[Ca^{2+}]_{cyt}$ does not appear to be a second messenger in the sensing of Pi in either Pi-replete Arabidopsis roots (Demidchik et al., 2003) or Pi-starved roots (this study), its use is altered when Pi supply is limited. In addition to elucidating the mechanistic basis of these altered signatures in response to abiotic stress and determining downstream consequences for signalling, it is also now appropriate to investigate the impact of nutritional status on Ca^{2+} signalling in biotic interactions.

MATERIAL & METHODS

Plant materials and growth conditions

All plant material used was in the Arabidopsis (*Arabidopsis thaliana*) ecotype Col-0 background, stably transformed with constitutively expressed cytosolic (apo)aequorin (pMAQ2, Knight et al., 1991) or the cytosolic sensor Yellow Cameleon 3.6 (NES-YC3.6, Krebs et al., 2012). Surface-sterilized seeds were sown aseptically on half-strength Murashige and Skoog (MS) growth medium including vitamins (Duchefa), with pH adjusted to 5.6 using KOH, and solidified using 0.8 % (w/v) agar (Bacto agar, BD Biosciences). Plates (12 cm x 12 cm, Greiner Bio-One) were sealed using micropore tape (3M) to allow for gas exchange. All seeds were stratified at 4°C and in darkness for 2 to 3 days prior to placing plates vertically into long-day conditions (16 h light / 8 h dark) in a growth chamber with 78 µmol m^{-2} s^{-1} light intensity, at 23°C (CLF Plant Climatics).

Standard half MS comprised the full phosphate ('full Pi') and full nitrogen ('full N') growth conditions. A custom-made MS medium without Pi was used for 'zero Pi' conditions (Duchefa, DU1072) or without N for 'zero N' conditions (PhytoTechnology Laboratories, M531). KCl was used to substitute for missing potassium (K^+) whenever Pi (KH_2PO_4) or N (KNO_3) were excluded**.** As the N-free medium was not available including vitamins, MS vitamin x 1000 stock solution (Sigma-Aldrich, M7150) was added to 'zero N' medium to the same final concentration. For all growth conditions requiring modified iron (Fe) or copper (Cu) content, half MS medium was prepared from stock solutions and vitamins were supplied from the MS vitamin x 1000 stock. For transfer experiments, 8-day-old seedlings were transferred to fresh growth medium plates, containing full/zero Pi growth medium (as described in the text), and grown for an additional 2 days.

Quantification of primary root length

Plates containing seedlings were scanned using a Perfection V300 Photo scanner (Epson) with 300-dpi resolution, saving the images in ".tiff" format. The software ImageJ (Abràmoff et al., 2004) and plug-in NeuronJ (Meijering et al., 2004) were used to trace primary root lengths.

Aequorin-based $[Ca^{2+}]_{cyt}$ measurements

Nutrient growth conditions were maintained throughout the experiments, *i.e.* all incubation and treatment solutions were prepared in the respective liquid half-strength MS medium, including 1.175 mM MES, adjusted to pH 5.6 using Tris. Excised primary root tips of 11-day-old Arabidopsis expressing (apo)aequorin were used for luminescence-based quantification of $[Ca^{2+}]_{cyt}$ dynamics, unless stated otherwise. Reconstitution of aequorin with coelenterazine (CTZ) *in vivo* was modified after Knight et al., 1997. In short, an excised tip was placed individually in a well of a white 96-well plate (Greiner Bio-One), incubated in 10 µM coelenterazine (NanoLight Technology) overnight, in darkness and at room temperature. A FLUOstar OPTIMA plate reader (BMG Labtech) was used to record baseline luminescence for 35 seconds, before injecting 100 µl of different treatment solutions with an injection speed of 150 µl s^{-1}. Changes in luminescence signal were monitored for 120 seconds, before injecting 100 µl of discharge solution (final concentration: 10 % (v/v) ethanol, 1 M $CaCl_2$) and monitoring for another 45 seconds. Concentrations of $[Ca^{2+}]_{cyt}$ were calculated as described (Knight et al., 1997). Treatments included the following: adenosine 5'-triphosphate disodium salt trihydrate (ATP, Melford); adenosine 5'-diphosphate disodium salt dehydrate (ADP, Melford); nonhydrolyzable ATP-analog adenosine 5'-[γ-thio]triphosphate tetralithium salt (γ-ATP, Sigma); phosphoric acid (Thermo Fisher); NaCl (Thermo Fisher); osmotic control for NaCl treatments, D-sorbitol (Sigma-Aldrich); hydrogen peroxide (H_2O_2, Sigma). The accompanying ions (Na^+ for ATP and ADP; Li^+ for γ-ATP) were previously shown in our laboratory not to confound the response

(Demidchik et al., 2009). Test treatments were pH adjusted to 5.6 using Tris and prepared at double strength, as in the well, a 1:2 dilution led to the desired final concentration. A Vapro5520 osmometer (Wescor) was used to check the osmolality of the NaCl and D-sorbitol treatment solutions.

Ratiometric $[Ca^{2+}]_{cyt}$ measurements

Ten-day-old Arabidopsis seedlings expressing NES-YC3.6 were mounted into a custom-built superfusion chamber (Behera and Kudla, 2013), stabilized with wetted cotton wool, and continuously superfused with imaging solution (IS; 5mM KCl, 10 mM $CaCl_2$, 10 mM MES, set to pH 5.8 using Tris; Loro et al., 2016) using an EconoPump system (Bio-Rad) with a tube diameter of 0.8 mm and a speed of 0.9 ml/minute. Seedlings were left to acclimatize to constant superfusion for 10 to 15 minutes, before starting an experiment. At the start of an experiment, seedlings were imaged for two minutes while superfusing IS. Extracellular ATP treatment (1 mM ATP, in IS background, pH 5.8) was then superfused over the roots for three minutes before changing back to IS without ATP. Images were captured using a Ti-E wide-field inverted fluorescence microscope (Nikon) with a Nikon Plan Fluor 4x 0.13 dry objective. The samples were excited at 440 nm using a Prior Lumen 200 PRO fluorescent light source (Prior Scientific). Images were collected with an ORCA-D2 Dual CCD camera (Hamamatsu) every five seconds for up to 30 minutes. NIS Elements AR 4.0 software (Nikon) was used to control the microscope, light source, and camera. ImageJ Fiji software was used to process the cpVenus and CFP fluorescence intensities. Using the 'Roi Manager' tool, each root sample was individually fitted with comparable ROIs. The *z* axis profiles were plotted for each channel, individually background subtracted, and used to calculate FRET (Förster resonance energy transfer) raw ratios (cpVenus/CFP). Normalization of data was carried out by taking into account differences in prestimulus baseline ($\Delta R/R_0 = R - R_0/R_0$, with R – cpVenus/CFP ratio, R_0 – averaged cpVenus/CFP prestimulus baseline ratio, after Loro et al., 2016).

ROS imaging

The membrane-permeable dye CM-H_2DCFDA (2', 7'-dichlorodihydrofluorescein diacetate, Thermo Fisher) was used at a final concentration of 20 µM, in assay medium (0.1 mM KCl, 0.1 mM $CaCl_2$, 1.175 mM MES, set to pH 6.0 using Tris; adapted from Foreman *et al*., 2003). Ten- to 11-day-old seedlings were incubated for 1 hour (dark, 4°C), gently washed in fresh assay medium without dye, and placed on plates containing growth medium maintaining previous growth conditions for 1 hour (light, RT) to acclimatize, before imaging primary root tips under a stereomicroscope, M205 FA (Leica), with a DFC365FX camera (Leica) and a Sola SE365 light source (Lumencor). Excitation at 470/40 nm was used and a GFP-ET filter collected emission at 525/50 nm, with a 400 ms exposure time, 70 % light intensity, and a gain of 2.0 and 50 x magnification. LAS X software (Leica) was used to control the microscope, light source, and camera. Image analysis was done using Fiji ImageJ software, tracing each root using the line tool (line width: 10) in combination with the 'plot profile' function, which reports signal intensity along the root (Reyt et al., 2015). For each root, three lines were drawn (from root apex shootwards through centre of root, from root apex shootwards along the upper side of the root, from root apex shootwards along the lower part of the root), and the intensity profiles were averaged per root (Reyt et al., 2015).

Data analysis

Data analysis and all statistical tests were performed using the open-source software R (www.r-project.org, version 3.5.1) in an R studio environment. The package 'MESS' was used to calculate area under the response curve. Analysis of variance (ANOVA) and Tukey's HSD *post-hoc* test were

469 employed to determine differences among the groups. A 95% family-wise confidence level was
470 applied.

471 **Accession Numbers**

472 Sequence data from this article can be found in the GenBank/EMBL data libraries under accession
473 numbers M11394.1 (aequorin) and AB178712 (YC3.6).

474 **Supplemental Data**

475 Supplemental Figure S1. Schematic representation of aequorin-based $[Ca^{2+}]_{cyt}$ time-course analyses.

476 Supplemental Figure S2. The $[Ca^{2+}]_{cyt}$ response of nitrogen-starved root tips to salt and osmotic
477 stress.

478 Supplemental Figure S3. The $[Ca^{2+}]_{cyt}$ response of Pi-starved root tips to mechanical stimulation and a
479 Pi source.

480 Supplemental Figure S4. The $[Ca^{2+}]_{cyt}$ response of Pi-starved root tips to extracellular ADP.

481 Supplemental Figure S5. The $[Ca^{2+}]_{cyt}$ response of Pi-starved root tips to a non-hydrolysable ATP
482 analog.

483 Supplemental Figure S6. The $[Ca^{2+}]_{cyt}$ response of Pi-starved root tips to oxidative stress.

484 Supplemental Figure S7. The $[Ca^{2+}]_{cyt}$ response of nitrogen-starved root tips to extracellular ATP.

485 Supplemental Figure S8. The $[Ca^{2+}]_{cyt}$ response of nitrogen-starved root tips to oxidative stress.

486 Supplemental Figure S9. The $[Ca^{2+}]_{cyt}$ response of copper- and Pi-starved root tips to extracellular
487 ATP.

488 Supplemental Table S1. Mean primary root lengths of Arabidopsis plants used in this study.

489 Supplemental Movie S1. Ratiometric false-color movie from a representative time series of a Pi-
490 replete Col-0 root expressing NES-YC3.6, response to 1 mM extracellular ATP.

491 Supplemental Movie S2. Ratiometric false-color movie from a representative time series of a Pi-
492 starved Col-0 root expressing NES-YC3.6, response to 1 mM extracellular ATP.

493

494

495

ACKNOWLEDGEMENTS

Financial support from the BBSRC (BB/J014540/1), the Broodbank Trust, Ministero dell'Istruzione dell'Università e della Ricerca, Fondo per gli Investimenti della Ricerca di Base (FIRB) 2010 RBFR10S1LJ_001, University of Milan Transition Grant - Horizon 2020, Fondo di ricerca Linea 1A Progetto "Unimi Partenariati H2020" and Piano di Sviluppo di Ateneo 2016, 2017 is gratefully acknowledged. We thank Adeeba Dark (University of Cambridge) and Laura Luoni (University of Milan) for technical support and training, and Alex Webb (University of Cambridge) for useful discussions.

506 **FIGURE LEGENDS**

507 **Figure 1. Pi-starved root tips have a dampened $[Ca^{2+}]_{cyt}$ response to mechanical, salt, and osmotic**
508 **stress.** Arabidopsis Col-0 aequorin-expressing seedlings were grown on full, medium (med), or zero
509 Pi (green, purple, and blue traces, respectively). Individual root tips (1 cm) of 11-day-old seedlings
510 were challenged with treatments applied at 35 seconds (black arrow), and $[Ca^{2+}]_{cyt}$ was measured for
511 155 seconds. (A) Mechanical stimulation (control solution); time course trace represents mean ±
512 standard error of mean (SEM) from 18 independent trials, with n = 150 - 155 root tips per growth
513 condition averaged per data point. Time-course data were analyzed for (B) touch maxima and (C)
514 area under the response curve (AUC), both baseline-subtracted, with each dot representing an
515 individual data point (see Supplemental Fig. S1 for details). The middle line in the box plot denotes
516 the median. (D-F) Responses to 150 mM NaCl (3 independent trials, n = 35 – 36 root tips). (G-I)
517 Responses to 280 mM sorbitol (3 independent trials, n = 22 - 24 root tips). Analysis of variance
518 (ANOVA) with *post-hoc* Tukey's test was used to assess statistical differences; different lowercase
519 letters denote significant differences ($p < 0.05$).

520

521 **Figure 2. Pi-starved root tips show a dampened $[Ca^{2+}]_{cyt}$ response to extracellular ATP.** Arabidopsis
522 Col-0 aequorin-expressing seedlings were grown on full, medium (med), or zero Pi (green, purple,
523 and blue traces, respectively). Individual root tips (1 cm) of 11-day-old seedlings were challenged
524 with treatments applied at 35 seconds (black arrow), and $[Ca^{2+}]_{cyt}$ was measured for 155 seconds. (A)
525 Treatment with 0.1 mM ATP; time-course trace represents mean ± standard error of mean (SEM)
526 from 6 independent trials, with n = 34 - 36 individual root tips averaged per data point. Time-course
527 data were analyzed for (B) touch maxima, (C) Peak 1 maxima, (D) Peak 2 maxima, and (E) area under
528 the response curve (AUC), all baseline-subtracted, with each dot representing an individual data
529 point (see Supplementary Fig. S1 for details). The middle line in the box plot denotes the median. (F-
530 J) Responses to 1 mM ATP (5 independent trials, n = 27 - 45 root tips per growth condition). Analysis
531 of variance (ANOVA) with *post-hoc* Tukey's test was used to assess statistical differences; different
532 lowercase letters denote significant differences ($p < 0.05$).

533

534 **Figure 3. eATP elicits two spatiotemporally distinct $[Ca^{2+}]_{cyt}$ increases in the root, which are altered**
535 **by Pi starvation.** (A) Representative full Pi-grown Arabidopsis Col-0 root expressing NES-YC3.6.
536 White dashed line in root micrograph indicates line used for kymograph extraction; scale bar: 1 mm.
537 (B) Kymograph depicts temporal and spatial changes in $[Ca^{2+}]_{cyt}$ of a representative full Pi-grown root
538 in response to a 3-minute 1 mM eATP treatment (purple bar), preceded and followed by superfusion
539 with control imaging solution. (C, D) Representative zero-Pi-grown root. White triangles indicate
540 secondary increase in $[Ca^{2+}]_{cyt}$ in the full Pi root, which is missing in the zero Pi root (marked by white
541 star).

542

543 **Figure 4. Quantification of differential $[Ca^{2+}]_{cyt}$ response of Pi-starved roots to eATP.** Arabidopsis
544 Col-0 expressing the cytosolic Yellow Cameleon 3.6 (NES-YC3.6) was grown on full or zero Pi. In a
545 superfusion chamber, a root of a 10-day-old seedling was superfused with imaging solution before
546 switching to 1 mM eATP (applied during 50 – 230 second interval after start of image acquisition,
547 purple shading), followed by washout with imaging solution. On the left, representative root with
548 annotated ROIs ("Roi", white boxes), analyzed and plotted over time in A – H, scale bar: 1 mm. (A, B):
549 Roi D; (C, D): Roi C; (E, F): Roi B; (G, H): Roi A. (A, C, E, G) Mean FRET ratio (cpVenus/CFP) ± SEM,

background subtracted; (B, D, F, H) normalized FRET ratio ($\Delta R/R_0$) ± SEM, of full Pi (green trace) and zero Pi roots (blue trace). Data from 3 independent trials, with n = 7 - 9 individual roots per growth condition.

Figure 5. Pi starvation modulates the root tip $[Ca^{2+}]_{cyt}$ response to eATP during development. Arabidopsis Col-0 aequorin-expressing seedlings were grown on full or zero Pi (green and blue traces, respectively). Root tips (1 cm) of (A) 6-day-old, (B) 7-day-old, (C) 8-day-old, or (D) 11-day-old seedlings were challenged with 1 mM eATP applied at 35 seconds (black arrow), and $[Ca^{2+}]_{cyt}$ was measured for 155 seconds. Time-course trace represents mean ± standard error of mean (SEM) from 3 - 5 independent trials, with n = 13 - 45 individual root tips averaged per data point. Time-course data were analyzed for (E) area under the response curve, baseline-subtracted, with each dot representing an individual data point; see Supplemental Fig. S1 for details. The middle line in the box plot in (E) denotes the median. Analysis of variance (ANOVA) with *post-hoc* Tukey's test was used to assess statistical differences. Different lowercase letters indicate groups of significant statistical difference ($p < 0.05$); same letters indicate no statistical significance ($p > 0.05$).

Figure 6. Resupply of Pi to Pi-starved seedlings rescues the dampened root tip $[Ca^{2+}]_{cyt}$ response to eATP. Arabidopsis Col-0 expressing aequorin was grown on zero Pi for 8 days, when plants were (i) not transferred ('zero Pi no transfer'), (ii) transferred to zero Pi growth medium ('zero Pi to zero Pi'), or (iii) transferred to full Pi growth medium ('zero Pi to full Pi'). After 2 days, individual excised root tips (1 cm) were challenged with treatments applied at 35 seconds (black arrow), and $[Ca^{2+}]_{cyt}$ was measured for 155 seconds. (A) Application of 1 mM ATP; time-course trace represents mean ± standard error of mean (SEM) from 3 independent trials, with n = 15 - 28 individual root tips averaged per data point. Time-course data were analyzed for (B) touch maxima, (C) Peak 1 maxima, (D) Peak 2 maxima, and (E) area under the response curve (AUC), all baseline-subtracted, with each dot representing an individual data point (see Supplementary Fig. S1 for details). The middle line in the box plot denotes the median. Analysis of variance (ANOVA) with *post-hoc* Tukey's test was used to assess statistical differences; different lowercase letters indicate significant differences ($p < 0.05$).

Figure 7. Iron levels modify the $[Ca^{2+}]_{cyt}$ response of Pi-starved root apices to eATP. Arabidopsis Col-0 aequorin-expressing seedlings were grown on standard half-strength MS growth medium, full Pi-full Fe (green trace), zero Pi-full Fe (blue trace), zero Pi-low Fe (pink trace), or zero Pi-zero Fe (orange trace). Excised root apices (1 cm) of 11-day-old seedlings were challenged with treatments applied at 35 seconds (black arrow), and $[Ca^{2+}]_{cyt}$ was measured for 155 seconds. (A) Application of 1 mM eATP; time-course trace represents mean ± standard error of mean (SEM) from 3 - 6 independent trials, with n = 24 - 61 individual root tips averaged per data point. Time-course data were analyzed for (B) touch maxima, (C) Peak 1 maxima, (D) Peak 2 maxima, and (E) area under the response curve (AUC), all baseline-subtracted, with each dot representing an individual data point (see Supplemental Fig. S1 for details). The middle line in the box plot denotes the median. Analysis of variance (ANOVA) with *post-hoc* Tukey's test was used to assess statistical differences; different lowercase letters indicate significant differences ($p < 0.05$).

Figure 8. Intracellular ROS are modified by Pi and Fe availability and influence root $[Ca^{2+}]_{cyt}$ response to eATP. Ten- to 11-day-old Arabidopsis Col-0 grown on (A,B) full Pi-full Fe, (C,D) zero Pi-full Fe, and (E,F) zero Pi-zero Fe were stained for intracellular ROS using 20 µM CM-H_2DCFDA, (G,H) nonstained control root, (A,C,E,G) representative bright-field images, and (B,D,F,H) representative false-colored fluorescence images; scale bar in (A,B) 1 mm. (I) Fluorescence intensity was quantified, background subtracted, and averaged along the root length. Mean values (colored lines) ± SEM (grey shading) are shown; data from 3 independent trials, with n = 14 - 16 roots analyzed per growth condition.

602

Parsed Citations

Abel S (2017) 'Phosphate scouting by root tips', Current Opinion in Plant Biology. pp. 168–177. doi: 10.1016/j.pbi.2017.04.016.
Pubmed: Author and Title
Google Scholar: Author Only Title Only Author and Title

Abràmoff MD, Hospitals I, Magalhães PJ and Abràmoff M (2004) 'Image Processing with ImageJ', Biophotonics International.

Andersson MX, Larsson KE, Tjellström H, Liljenberg C and Sandelius AS (2005) 'Phosphate-limited oat: The plasma membrane and the tonoplast as major targets for phospholipid-to-glycolipid replacement and stimulation of phospholipases in the plasma membrane', Journal of Biological Chemistry, 280, pp. 27578–27586. doi: 10.1074/jbc.M503273200.
Pubmed: Author and Title
Google Scholar: Author Only Title Only Author and Title

Balzergue C, Dartevelle T, Godon C, Laugier E, Meisrimler C, Teulon J-M, Creff A, Bissler M, Brouchoud C, Hagège A, et al. (2017) 'Low phosphate activates STOP1-ALMT1 to rapidly inhibit root cell elongation', Nature Communication, doi: 10.1038/ncomms15300.
Pubmed: Author and Title
Google Scholar: Author Only Title Only Author and Title

Behera S, Long Y, Schmitz-Thom I, Wang X-P, Zhang C, Li H, Steinhorst L, Manishankar P, Ren X-L, Offenborn JN, et al. (2017) 'Two spatially and temporally distinct Ca2+ signals convey Arabidopsis thaliana responses to K+ deficiency', New Phytologist, 213, pp. 739–750. doi: 10.1111/nph.14145.
Pubmed: Author and Title
Google Scholar: Author Only Title Only Author and Title

Behera S, Zhaolong X, Luoni L, Bonza MC, Doccula FG, Michelis MI De, Morris RJ, Costa A and Centre JI (2018) 'Cellular Ca2+ signals generate defined pH signatures in plants', Plant Cell. doi: 10.1105/tpc.18.00655.
Pubmed: Author and Title
Google Scholar: Author Only Title Only Author and Title

Behera S and Kudla J (2013) 'High-resolution imaging of cytoplasmic Ca2+ dynamics in Arabidopsis roots', Cold Spring Harbor Protocols, 8, pp. 670–674. doi: 10.1101/pdb.prot073023.
Pubmed: Author and Title
Google Scholar: Author Only Title Only Author and Title

Bonza MC, Loro G, Behera S, Wong A, Kudla J and Costa A (2013) 'Analyses of Ca2+ accumulation and dynamics in the endoplasmic reticulum of Arabidopsis root cells using a genetically encoded cameleon sensor', Plant Physiology, 163, pp. 1230–41. doi: 10.1104/pp.113.226050.
Pubmed: Author and Title
Google Scholar: Author Only Title Only Author and Title

Chen D, Cao Y, Li H, Kim D, Ahsan N, Thelen J and Stacey G (2017) 'Extracellular ATP elicits DORN1-mediated RBOHD phosphorylation to regulate stomatal aperture', Nature Communications. doi: 10.1038/s41467-017-02340-3.
Pubmed: Author and Title
Google Scholar: Author Only Title Only Author and Title

Chien P-S, Chiang C-P, Leong SJ and Chiou T-J (2018) 'Sensing and signaling of phosphate starvation – from local to long distance', Plant and Cell Physiology, 59. doi: 10.1093/pcp/pcy148.
Pubmed: Author and Title
Google Scholar: Author Only Title Only Author and Title

Chiou T-J and Lin S-I (2011) 'Signaling network in sensing phosphate availability in plants', Annual Review of Plant Biology, 62, pp. 185–206. doi: 10.1146/annurev-arplant-042110-103849.
Pubmed: Author and Title
Google Scholar: Author Only Title Only Author and Title

Choi J, Tanaka K, Cao Y, Qi Y, Qiu J, Liang Y, Lee SY and Stacey G (2014) 'Identification of a plant receptor for extracellular ATP', Science, 343, pp. 290–4. doi: 10.1126/science.343.6168.290.
Pubmed: Author and Title
Google Scholar: Author Only Title Only Author and Title

Cole CV, Olsen SR, Scott CO (1953) 'The nature of phosphate sorption by calcium carbonate', Proceedings of the Soil Science Society of America, 135, pp. 352-356.
Pubmed: Author and Title
Google Scholar: Author Only Title Only Author and Title

Conn S and Gilliham M (2010) 'Comparative physiology of elemental distributions in plants', Annals of Botany, 105, pp. 1081–1102. doi: 10.1093/aob/mcq027.
Pubmed: Author and Title
Google Scholar: Author Only Title Only Author and Title

Costa A, Candeo A, Fieramonti L, Valentini G and Bassi A (2013) 'Calcium dynamics in root cells of Arabidopsis thaliana visualized with Selective Plane Illumination Microscopy', PLoS ONE. doi: 10.1371/journal.pone.0075646.
Pubmed: Author and Title

Google Scholar: Author Only Title Only Author and Title

Dark A, Demidchik V, Shabala S and Davies JM (2011) 'Release of extracellular purines from plant roots and effect on ion fluxes', Plant Signaling and Behavior, 6, pp. 1855–1857. doi: 10.1093/jxb/ern242.5.
Pubmed: Author and Title
Google Scholar: Author Only Title Only Author and Title

Demidchik V, Nichols C, Oliynyk M, Dark A, Glover BJ and Davies JM (2003) 'Is ATP a signaling agent in plants?', Plant Physiology, 133, pp. 456–461. doi: 10.1104/pp.103.024091.1978.
Pubmed: Author and Title
Google Scholar: Author Only Title Only Author and Title

Demidchik V, Shang Z, Shin R, Thompson E, Rubio L, Laohavisit A, Mortimer JC, Chivasa S, Slabas AR, Glover BJ, et al. (2009) 'Plant extracellular ATP signalling by plasma membrane NADPH oxidase and Ca2+ channels', Plant Journal, 58, pp. 903–913. doi: 10.1111/j.1365-313X.2009.03830.x.
Pubmed: Author and Title
Google Scholar: Author Only Title Only Author and Title

Demidchik V, Shang Z, Shin R, Colaço R, Laohavisit A, Shabala S and Davies JM (2011) 'Receptor-like activity evoked by extracellular ADP in Arabidopsis root epidermal plasma membrane', Plant Physiology, 156, pp. 1375–1385. doi: 10.1104/pp.111.174722.
Pubmed: Author and Title
Google Scholar: Author Only Title Only Author and Title

Demidchik V (2018) 'ROS-activated ion channels in plants: Biophysical characteristics, physiological functions and molecular nature', International Journal of Molecular Sciences, 19, pp. 17–21. doi: 10.3390/ijms19041263.
Pubmed: Author and Title
Google Scholar: Author Only Title Only Author and Title

Demidchik V, Shabala SN and Davies JM (2007) 'Spatial variation in H2O2 response of Arabidopsis thaliana root epidermal Ca2+ flux and plasma membrane Ca2+ channels', Plant Journal, 49, pp. 377–386. doi: 10.1111/j.1365-313X.2006.02971.x.
Pubmed: Author and Title
Google Scholar: Author Only Title Only Author and Title

Duan G, Walther D and Schulze WX (2013) 'Reconstruction and analysis of nutrient-induced phosphorylation networks in Arabidopsis thaliana', Frontiers in Plant Science. doi: 10.3389/fpls.2013.00540.
Pubmed: Author and Title
Google Scholar: Author Only Title Only Author and Title

Duff SM, Moorhead GB, Lefebvre DD and Plaxton WC (1989) 'Phosphate starvation inducible "Bypasses" of adenylate and phosphate dependent glycolytic enzymes in Brassica nigra suspension cells', Plant Physiology, 90, pp. 1275–1278. doi: 10.1104/pp.90.4.1275.
Pubmed: Author and Title
Google Scholar: Author Only Title Only Author and Title

Edel KH and Kudla J (2015) 'Increasing complexity and versatility: how the calcium signaling toolkit was shaped during plant land colonization', Cell Calcium, 57, pp. 231–46. doi: 10.1016/j.ceca.2014.10.013.
Pubmed: Author and Title
Google Scholar: Author Only Title Only Author and Title

Ensikat H-J, Geisler T and Weigend M (2016) 'A first report of hydroxylated apatite as structural biomineral in Loasaceae-plants' teeth against herbivores', Scientific Reports. doi: 10.1038/srep26073.
Pubmed: Author and Title
Google Scholar: Author Only Title Only Author and Title

Foreman J, Demidchik V, Bothwell JHF, Mylona P, Miedema H, Torresk MA, Linstead P, Costa S, Brownlee C, Jones JDG, et al. (2003) 'Reactive oxygen species produced by NADPH oxidase regulate plant cell growth', Nature, 422, pp. 442–446.
Pubmed: Author and Title
Google Scholar: Author Only Title Only Author and Title

Gleason C, Huang S, Thatcher LF, Foley RC, Anderson CR, Carroll AJ, Millar AH, Singh KB (2011) 'Mitochondrial complex II has a key role in mitochondrial-derived reactive oxygen species influence on plant stress gene regulation and defense', Proceedings of the National Academy of Sciences USA, 108, pp.10768-10773. doi: 10.1073/pnas.1016060108.
Pubmed: Author and Title
Google Scholar: Author Only Title Only Author and Title

Gruber BD, Giehl RFH, Friedel S and von Wirén N (2013) 'Plasticity of the Arabidopsis root system under nutrient deficiencies', Plant Physiology, 163, pp. 161–79. doi: 10.1104/pp.113.218453.
Pubmed: Author and Title
Google Scholar: Author Only Title Only Author and Title

Hoehenwarter W, Mönchgesang S, Neumann S, Majovsky P, Abel S and Müller J (2016) 'Comparative expression profiling reveals a role of the root apoplast in local phosphate response', BMC Plant Biology. doi: 10.1186/s12870-016-0790-8.
Pubmed: Author and Title
Google Scholar: Author Only Title Only Author and Title

Kawa D, Julkowska M, Montero Sommerfeld H, Borst Ter, Haring MA and Testerink C (2016) 'Phosphate-dependent root system

architecture responses to salt stress', Plant Physiology, 172, p. pp.00712.2016. doi: 10.1104/pp.16.00712.
Pubmed: Author and Title
Google Scholar: Author Only Title Only Author and Title

Kellermeier F, Armengaud P, Seditas TJ, Danku J, Salt DE and Amtmann A (2014) 'Analysis of the root system architecture of Arabidopsis provides a quantitative readout of crosstalk between nutritional signals', Plant Cell, 26, pp. 1480–1496. doi: 10.1105/tpc.113.122101.
Pubmed: Author and Title
Google Scholar: Author Only Title Only Author and Title

Kiegle E, Moore CA, Haseloff J, Tester MA and Knight MR (2000) 'Cell-type-specic calcium responses to drought , salt and cold in the Arabidopsis root', The Plant Journal, 23, pp. 267–278.
Pubmed: Author and Title
Google Scholar: Author Only Title Only Author and Title

Kim S-Y, Sivaguru M and Stacey G (2006) 'Extracellular ATP in plants. Visualization, localization, and analysis of physiological significance in growth and signaling', Plant Physiology, 142, pp. 984–992. doi: 10.1104/pp.106.085670.
Pubmed: Author and Title
Google Scholar: Author Only Title Only Author and Title

Knight H, Trewavas AJ and Knight MR (1997) 'Calcium signalling in Arabidopsis thaliana responding to drought and salinity', The Plant Journal, 12, pp. 1067–1078.
Pubmed: Author and Title
Google Scholar: Author Only Title Only Author and Title

Knight MR, Campbell AK, Smith SM and Trewavas AJ (1991) 'Transgenic plant aequorin reports the effects of touch and cold-shock and elicitors on cytoplasmic calcium', Nature, 352, pp. 524–526. doi: 10.1038/352524a0.
Pubmed: Author and Title
Google Scholar: Author Only Title Only Author and Title

Knight MR, Smith SM and Trewavas AJ (1992) 'Wind-induced plant motion immediately increases cytosolic calcium', Proceedings of the National Academy of Sciences USA, 89, pp. 4967–4971. doi: 10.1073/pnas.89.11.4967.
Pubmed: Author and Title
Google Scholar: Author Only Title Only Author and Title

Knight H, Trewavas AJ and Knight MR (1997) 'Recombinant aequorin methods for measurement of intracellular calcium in plants', Plant Molecular Biology Manual, pp.1-22

Koshiba T, Kobayashi M, Ishihara A and Matoh T (2010) 'Boron nutrition of cultured Tobacco BY-2 Cells. VI. calcium is involved in early responses to boron deprivation', Plant and Cell Physiology, 51, pp. 323–327. doi: 10.1093/pcp/pcp179.
Pubmed: Author and Title
Google Scholar: Author Only Title Only Author and Title

Krebs M, Held K, Binder A, Hashimoto K, Den Herder G, Parniske M, Kudla J and Schumacher K (2012) 'FRET-based genetically encoded sensors allow high-resolution live cell imaging of Ca2+ dynamics', Plant Journal, 69, pp. 181–192. doi: 10.1111/j.1365-313X.2011.04780.x.
Pubmed: Author and Title
Google Scholar: Author Only Title Only Author and Title

Lan P, Li W and Schmidt W (2012) 'Complementary proteome and transcriptome profiling in phosphate-deficient Arabidopsis roots reveals multiple levels of gene regulation', Molecular and Cellular Proteomics, 11, pp. 1156–1166. doi: 10.1074/mcp.M112.020461.
Pubmed: Author and Title
Google Scholar: Author Only Title Only Author and Title

Laohavisit A, Shang Z, Rubio L, Cubin TA, Very A-A, Wang A, Mortimer JC, Macpherson N, Coxon KM, Battey NH, et al. (2012) 'Arabidopsis Annexin1 mediates the radical-activated plasma membrane Ca2+- and K+-permeable conductance in root cells', Plant Cell, 24, pp. 1522–1533. doi: 10.1105/tpc.112.097881.
Pubmed: Author and Title
Google Scholar: Author Only Title Only Author and Title

Laohavisit A, Richards SL, Shabala L, Chen C, Colaco RDDR, Swarbreck SM, Shaw E, Dark A, Shabala S, Shang Z, et al. (2013) 'Salinity-induced calcium signaling and root adaptation in Arabidopsis require the calcium regulatory protein annexin 1', Plant Physiology, 163, pp. 253–262. doi: 10.1104/pp.113.217810.
Pubmed: Author and Title
Google Scholar: Author Only Title Only Author and Title

Lenzoni G, Liu J and Knight MR (2017) 'Predicting plant immunity gene expression by identifying the decoding mechanism of calcium signatures', New Phytologist. doi: 10.1111/nph.14924.
Pubmed: Author and Title
Google Scholar: Author Only Title Only Author and Title

Lin W-D, Liao Y-Y, Yang TJW, Pan C-Y, Buckhout TJ and Schmidt W (2011) 'Coexpression-based clustering of Arabidopsis root genes predicts functional modules in early phosphate deficiency signaling', Plant Physiology, 155, pp. 1383–1402. doi: 10.1104/pp.110.166520.
Pubmed: Author and Title

Google Scholar: Author Only Title Only Author and Title

Linn J, Ren M, Berkowitz O, Ding W, van der Merwe MJ, Whelan J and Jost R (2017) 'Root cell-specific regulators of phosphate-dependent growth', Plant Physiology, 174, pp. 1969–1989. doi: 10.1104/pp.16.01698.
Pubmed: Author and Title
Google Scholar: Author Only Title Only Author and Title

Liu J, Whalley HJ and Knight MR (2015) 'Combining modelling and experimental approaches to explain how calcium signatures are decoded by calmodulin-binding transcription activators (CAMTAs) to produce specific gene expression responses', New Phytologist, 208, pp. 174–187. doi: 10.1111/nph.13428.
Pubmed: Author and Title
Google Scholar: Author Only Title Only Author and Title

Liu K, Niu Y, Konishi M, Wu Y, Du H, Sun Chung H, Li L, Boudsocq M, McCormack M, Maekawa S, et al. (2017) 'Discovery of nitrate–CPK–NLP signalling in central nutrient–growth networks', Nature. doi: 10.1038/nature22077.
Pubmed: Author and Title
Google Scholar: Author Only Title Only Author and Title

Loro G, Drago I, Pozzan T, Schiavo F Lo, Zottini M and Costa A (2012) 'Targeting of Cameleons to various subcellular compartments reveals a strict cytoplasmic/mitochondrial Ca2+ handling relationship in plant cells', Plant Journal, 71, pp. 1–13. doi: 10.1111/j.1365-313X.2012.04968.x.
Pubmed: Author and Title
Google Scholar: Author Only Title Only Author and Title

Loro G, Wagner S, Doccula FG, Behera S, Weinl S, Kudla J, Schwarzländer M, Costa A and Zottini M (2016) 'Chloroplast-specific in vivo Ca2+ imaging using Yellow Cameleon fluorescent protein sensors reveals organelle-autonomous Ca2+ signatures in the stroma', Plant Physiology. doi: 10.1104/pp.16.00652.
Pubmed: Author and Title
Google Scholar: Author Only Title Only Author and Title

Manishankar P, Wang N, Köster P, Alatar AA and Kudla J (2018) 'Calcium signaling during salt stress and in the regulation of ion homeostasis', Journal of Experimental Botany, 61, pp. 302–320. doi: 10.1093/jxb/ery201.
Pubmed: Author and Title
Google Scholar: Author Only Title Only Author and Title

Marti MC, Stancombe MA and Webb AAR (2013) 'Cell- and stimulus type-specific intracellular free Ca2+ signals in Arabidopsis', Plant Physiology, 163, pp. 625–634. doi: 10.1104/pp.113.222901.
Pubmed: Author and Title
Google Scholar: Author Only Title Only Author and Title

Meijering E, Jacob M, Sarria JF, Steiner P, Hirling H and Unser M (2004) 'Design and validation of a tool for neurite tracing and analysis in fluorescence microscopy images', Cytometry, 58, pp. 167–176.
Pubmed: Author and Title
Google Scholar: Author Only Title Only Author and Title

Misson J, Raghothama KG, Jain A, Jouhet J, Block M a, Bligny R, Ortet P, Creff A, Somerville S, Rolland N, et al. (2005) 'A genome-wide transcriptional analysis using Arabidopsis thaliana Affymetrix gene chips determined plant responses to phosphate deprivation', Proceedings of the National Academy of Sciences USA, 102, pp. 11934–11939. doi: 10.1073/pnas.0505266102.
Pubmed: Author and Title
Google Scholar: Author Only Title Only Author and Title

Monshausen GB, Bibikova TN, Weisenseel MH and Gilroy S (2009) 'Ca2+ regulates reactive oxygen species production and pH during mechanosensing in Arabidopsis roots', The Plant Cell, 21, pp. 2341–56. doi: 10.1105/tpc.109.068395.
Pubmed: Author and Title
Google Scholar: Author Only Title Only Author and Title

Müller J, Toev T, Heisters M, Teller J, Moore KL, Hause G, Dinesh DC, Bürstenbinder K and Abel S (2015) 'Iron-dependent callose deposition adjusts root meristem maintenance to phosphate availability', Developmental Cell, 33, pp. 216–230. doi: 10.1016/j.devcel.2015.02.007.
Pubmed: Author and Title
Google Scholar: Author Only Title Only Author and Title

Mustafa A, Ensikat H-J and Weigend M (2018) 'Mineralized trichomes in Boraginales: complex microscale heterogeneity and simple phylogenetic patterns', Annals of Botany. doi: 10.1093/aob/mcx191.
Pubmed: Author and Title
Google Scholar: Author Only Title Only Author and Title

Nakamura Y (2013) 'Phosphate starvation and membrane lipid remodeling in seed plants', Progress in Lipid Research, 52, pp. 43–50. doi: 10.1016/j.plipres.2012.07.002.
Pubmed: Author and Title
Google Scholar: Author Only Title Only Author and Title

Okazaki Y, Otsuki H, Narisawa T, Kobayashi M, Sawai S, Kamide Y, Kusano M, Aoki T, Hirai MY and Saito K (2013) 'A new class of plant lipid is essential for protection against phosphorus depletion', Nature Communications. doi: 10.1038/ncomms2512.

Pubmed: Author and Title
Google Scholar: Author Only Title Only Author and Title

Pant B-D, Pant P, Erban A, Huhman D, Kopka J and Scheible W-R (2015) 'Identification of primary and secondary metabolites with phosphorus status-dependent abundance in Arabidopsis, and of the transcription factor PHR1 as a major regulator of metabolic changes during phosphorus-limitation', Plant, Cell and Environment, 38, pp. 172–187. doi: 10.1111/pce.12378.
Pubmed: Author and Title
Google Scholar: Author Only Title Only Author and Title

Peret B, Desnos T, Jost R, Kanno S, Berkowitz O and Nussaume L (2014) 'Root architecture responses: In search of phosphate', Plant Physiology, 166, pp. 1713–1723. doi: 10.1104/pp.114.244541.
Pubmed: Author and Title
Google Scholar: Author Only Title Only Author and Title

Plattner H and Verkhratsky A (2015) 'The ancient roots of calcium signalling evolutionary tree', Cell Calcium, 57, pp. 123–132. doi: 10.1016/j.ceca.2014.12.004.
Pubmed: Author and Title
Google Scholar: Author Only Title Only Author and Title

Plaxton WC and Tran HT (2011) 'Metabolic adaptations of phosphate-starved plants', Plant Physiology, 156, pp. 1006–1015. doi: 10.1104/pp.111.175281.
Pubmed: Author and Title
Google Scholar: Author Only Title Only Author and Title

Pratt J, Boisson A-M, Gout E, Bligny R, Douce R and Aubert S (2009) 'Phosphate (Pi) starvation effect on the cytosolic Pi concentration and Pi exchanges across the tonoplast in plant cells: an in vivo 31P-nuclear magnetic resonance study using methylphosphonate as a Pi analog', Plant Physiology, 151, pp. 1646–57. doi: 10.1104/pp.109.144626.
Pubmed: Author and Title
Google Scholar: Author Only Title Only Author and Title

Price AH, Taylor A, Ripley SJ, Griffiths A, Trewavas AJ and Knight MR (1994) 'Oxidative signals in tobacco increase cytosolic calcium', The Plant Cell, 6, pp. 1301–1310. doi: 10.1105/tpc.6.9.1301.
Pubmed: Author and Title
Google Scholar: Author Only Title Only Author and Title

Quiles-Pando C, Rexach J, Navarro-Gochicoa MT, Camacho-Cristóbal JJ, Herrera-Rodríguez MB and González-Fontes A (2013) 'Boron deficiency increases the levels of cytosolic Ca2+ and expression of Ca2+-related genes in Arabidopsis thaliana roots', Plant Physiology and Biochemistry, 65, pp. 55–60. doi: 10.1016/j.plaphy.2013.01.004.
Pubmed: Author and Title
Google Scholar: Author Only Title Only Author and Title

Quintero FJ, Martinez-Atienza J, Villalta I, Jiang X, Kim W-Y, Ali Z, Fujii H, Mendoza I, Yun D-J, Zhu J-K, et al. (2011) 'Activation of the plasma membrane Na+/H+ antiporter Salt-Overly-Sensitive 1 (SOS1) by phosphorylation of an auto-inhibitory C-terminal domain', Proceedings of the National Academy of Sciences USA, 108, pp. 2611–2616. doi: 10.1073/pnas.1018921108.
Pubmed: Author and Title
Google Scholar: Author Only Title Only Author and Title

Rentel MC and Knight MR (2004) 'Oxidative stress-induced calcium signaling in Arabidopsis', Plant Physiology, 135, pp. 1471–1479. doi: 10.1104/pp.104.042663.1.
Pubmed: Author and Title
Google Scholar: Author Only Title Only Author and Title

Reyt G, Boudouf S, Boucherez J, Gaymard F and Briat JF (2015) 'Iron- and ferritin-dependent reactive oxygen species distribution: Impact on Arabidopsis root system architecture', Molecular Plant, 8, pp. 439–453. doi: 10.1016/j.molp.2014.11.014.
Pubmed: Author and Title
Google Scholar: Author Only Title Only Author and Title

Richards SL, Laohavisit A, Mortimer JC, Shabala L, Swarbreck SM, Shabala S and Davies JM (2014) 'Annexin 1 regulates the H2O2-induced calcium signature in Arabidopsis thaliana roots', The Plant Journal, 77, pp. 136–45. doi: 10.1111/tpj.12372.
Pubmed: Author and Title
Google Scholar: Author Only Title Only Author and Title

Rincón-Zachary M, Teaster ND, Sparks JA, Valster AH, Motes CM and Blancaflor EB (2010) 'Fluorescence resonance energy transfer-sensitized emission of yellow cameleon 3.60 reveals root zone-specific calcium signatures in Arabidopsis in response to aluminum and other trivalent cations', Plant Physiology, 152, pp. 1442–58. doi: 10.1104/pp.109.147256.
Pubmed: Author and Title
Google Scholar: Author Only Title Only Author and Title

Riveras E, Alvarez JM, Vidal EA, Oses C, Vega A and Gutiérrez RA (2015) 'The calcium ion is a second messenger in the nitrate signaling pathway of Arabidopsis', Plant Physiology, 169, pp. 1397–404. doi: 10.1104/pp.15.00961.
Pubmed: Author and Title
Google Scholar: Author Only Title Only Author and Title

Song CJ, Steinebrunner I, Wang X, Stout SC and Roux SJ (2006) 'Extracellular ATP induces the accumulation of superoxide via NADPH oxidases in Arabidopsis', Plant Physiology, 140, pp. 1222–1232. doi: 10.1104/pp.105.073072.

Pubmed: Author and Title
Google Scholar: Author Only Title Only Author and Title

Svistoonoff S, Creff A, Reymond M, Sigoillot-Claude C, Ricaud L, Blanchet A, Nussaume L and Desnos T (2007) 'Root tip contact with low-phosphate media reprograms plant root architecture', Nature genetics, 39, pp. 792–796. doi: 10.1038/ng2041.
Pubmed: Author and Title
Google Scholar: Author Only Title Only Author and Title

Tanaka K, Gilroy S, Jones AM and Stacey G (2010) 'Extracellular ATP signaling in plants', Trends in Cell Biology, 20, pp. 601–8. doi: 10.1016/j.tcb.2010.07.005.
Pubmed: Author and Title
Google Scholar: Author Only Title Only Author and Title

Tanaka K, Swanson SJ, Gilroy S and Stacey G (2010) 'Extracellular nucleotides elicit cytosolic free calcium oscillations in Arabidopsis', Plant Physiology, 154, pp. 705–19. doi: 10.1104/pp.110.162503.
Pubmed: Author and Title
Google Scholar: Author Only Title Only Author and Title

Tang R-J, Zhao F-G, Garcia VJ, Kleist TJ, Yang L, Zhang H-X and Luan S (2015) 'Tonoplast CBL-CIPK calcium signaling network regulates magnesium homeostasis in Arabidopsis', Proceedings of the National Academy of Sciences of the United States of America, 112, pp. 3134–3139. doi: 10.1073/pnas.1420944112.
Pubmed: Author and Title
Google Scholar: Author Only Title Only Author and Title

Ticconi CA, Lucero RD, Sakhonwasee S, Adamson AW, Creff A, Nussaume L, Desnos T and Abel S (2009) 'ER-resident proteins PDR2 and LPR1 mediate the developmental response of root meristems to phosphate availability', Proceedings of the National Academy of Sciences of the United States of America, 106, pp. 14174–14179. doi: 10.1073/pnas.0901778106.
Pubmed: Author and Title
Google Scholar: Author Only Title Only Author and Title

Tjellstrom H, Hellgren LI, Wieslander A and Sandelius AS (2010) 'Lipid asymmetry in plant plasma membranes: phosphate deficiency-induced phospholipid replacement is restricted to the cytosolic leaflet', The FASEB Journal, 24, pp. 1128–1138. doi: 10.1096/fj.09-139410.
Pubmed: Author and Title
Google Scholar: Author Only Title Only Author and Title

Verkhratsky A and Parpura V (2015) 'Calcium signalling and calcium channels: Evolution and general principles', European Journal of Pharmacology. doi: 10.1016/j.ejphar.2013.11.013.Calcium.
Pubmed: Author and Title
Google Scholar: Author Only Title Only Author and Title

Vigani G and Briat J-F (2016) 'Impairment of respiratory chain under nutrient deficiency in plants: Does it play a role in the regulation of iron and sulfur responsive genes?', Frontiers in Plant Science, doi: 10.3389/fpls.2015.01185.
Pubmed: Author and Title
Google Scholar: Author Only Title Only Author and Title

Waadt R, Krebs M and Schumacher K (2017) 'Multiparameter imaging of calcium and abscisic acid and high-resolution quantitative calcium measurements using R-GECO1-mTurquoise in Arabidopsis', New Phytologist, 216, pp. 303–320. doi: 10.1111/nph.14706.
Pubmed: Author and Title
Google Scholar: Author Only Title Only Author and Title

Wang ZQ, Zhou X, Dong L, Guo J, Chen Y, Zhang Y, Wu L and Xu M (2018) 'iTRAQ-based analysis of the Arabidopsis proteome reveals insights into the potential mechanisms of anthocyanin accumulation regulation in response to phosphate deficiency', Journal of Proteomics. doi: 10.1016/j.jprot.2018.06.006.
Pubmed: Author and Title
Google Scholar: Author Only Title Only Author and Title

Ward JT, Lahner B, Yakubova E, Salt DE and Raghothama KG (2008) 'The effect of iron on the primary root elongation of Arabidopsis during phosphate deficiency', Plant Physiology, 147, pp. 1181–1191. doi: 10.1104/pp.108.118562.
Pubmed: Author and Title
Google Scholar: Author Only Title Only Author and Title

Weerasinghe RR, Swanson SJ, Okada SF, Garrett MB, Kim S-Y, Stacey G, Boucher RC, Gilroy S and Jones AM (2009) 'Touch induces ATP release in Arabidopsis roots that is modulated by the heterotrimeric G-protein complex', FEBS Letters, 583, pp. 2521–6. doi: 10.1016/j.febslet.2009.07.007.
Pubmed: Author and Title
Google Scholar: Author Only Title Only Author and Title

Weigend M, Mustafa A and Ensikat H-J (2017) 'Calcium phosphate in plant trichomes: the overlooked biomineral', Planta. doi: 10.1007/s00425-017-2826-1.
Pubmed: Author and Title
Google Scholar: Author Only Title Only Author and Title

Whalley HJ, Sargeant AW, Steele JFC, Lacoere T, Lamb R, Saunders NJ, Knight H and Knight MR (2011) 'Transcriptomic analysis

reveals calcium regulation of specific promoter motifs in Arabidopsis', The Plant Cell, 23, pp. 4079–4095. doi: 10.1105/tpc.111.090480.
Pubmed: Author and Title
Google Scholar: Author Only Title Only Author and Title

Whalley HJ and Knight MR (2013) 'Calcium signatures are decoded by plants to give specific gene responses', New Phytologist, 197, pp. 690–693. doi: 10.1111/nph.12087.
Pubmed: Author and Title
Google Scholar: Author Only Title Only Author and Title

Wilkins K, Matthus E, Swarbreck S and Davies JM (2016) 'Calcium-mediated abiotic stress signaling in roots', Frontiers in Plant Science. doi: 10.3389/fpls.2016.01296.
Pubmed: Author and Title
Google Scholar: Author Only Title Only Author and Title

Williamson LC, Ribrioux SP, Fitter AH and Leyser HM (2001) 'Phosphate availability regulates root system architecture in Arabidopsis', Plant Physiology, 126, pp. 875–882. doi: 10.1104/pp.126.2.875.
Pubmed: Author and Title
Google Scholar: Author Only Title Only Author and Title